AERO-ASTRONAUTICS REPORT NO. 29

LIFT-TO-DRAG RATIOS OF LIFTING BODIES AT HYPERSONIC SPEEDS

by

ANGELO MIELE and HO-YI HUANG

RICE UNIVERSITY

1967

CORRECTION TO THE REPORT AAR-29

With reference to the aerodynamic characteristics of a flat-bottom semiellipse, Eqs. (72) and (73) are valid only for $\alpha \geq 1$. For $\alpha \leq 1$, Eqs. (72) and (73) must be replaced by

$$J_1 = \alpha/\gamma^2 + \pi\alpha^2(\alpha + 4)/2(\alpha + 1)$$
$$- [\alpha^2(4 - 3\alpha^2)/\gamma^3] \arctan(\gamma/\alpha)$$

$$J_2 = \alpha + 1 + (1 - \gamma)\, F(\varphi, k) - (1 + \gamma)[1 - E(\varphi, k)] \qquad (72\text{-A})$$

$$J_3 = \alpha/\gamma^2 + \pi\alpha^2/(\alpha + 1) - [\alpha^2(2 - \alpha^2)/\gamma^3] \arctan(\gamma/\alpha)$$

where $\gamma = \sqrt{(1 - \alpha^2)}$. Here, F and E denote the incomplete elliptic integrals of the first and the second kind, whose argument φ and parameter k are given by

$$\varphi = \arctan[(1 + \gamma)/\alpha]$$
$$\qquad (73\text{-A})$$
$$k = 2\sqrt{\gamma}/(1 + \gamma)$$

LIFT-TO-DRAG RATIOS OF LIFTING BODIES AT HYPERSONIC SPEEDS[1]

by

ANGELO MIELE[2] and HO-YI HUANG[3]

SUMMARY

An investigation of the lift-to-drag ratio attainable by a slender, homothetic body flying at hypersonic speeds is presented under the assumptions that the pressure distribution is modified Newtonian and the surface-averaged skin-friction coefficient is constant. It is shown that a value of the thickness ratio exists such that the lift-to-drag ratio is a maximum; this particular value is such that the friction drag is one-third of the total drag. The subsequent optimization of the longitudinal contour is reduced to the extremization of the product of the powers of three integrals related to the lift, the pressure drag, and the skin-friction drag. In this connection, it is proved that a conical solution is the best.

---

[1] This research was supported by the NASA-Langley Research Center, Grant No. NGR-44-006-063.

[2] Professor of Astronautics and Director of the Aero-Astronautics Group, Department of Mechanical and Aerospace Engineering and Materials Science, Rice University, Houston, Texas.

[3] Graduate Student in Aero-Astronautics, Department of Mechanical and Aerospace Engineering and Materials Science, Rice University, Houston, Texas.

Concerning the transversal contour, a systematic analysis of the effect of the main geometric parameters of a cross section on the lift-to-drag ratio is presented. For a given elongation ratio, the following conclusions are derived: (a) the triangle is aerodynamically superior to the semiellipse and the rectangle, whether flat-top or flat-bottom; (b) the flat-bottom triangle is aerodynamically superior to the flat-top triangle; and (c) the diamond shape is better than the triangle, whether flat-top or flat-bottom.

1. INTRODUCTION

In previous papers (Refs. 1 and 2), the lift-to-drag ratio obtainable by a slender, flat-top, homothetic body at hypersonic speeds was studied under the assumptions that the pressure distribution is modified Newtonian and the surface-averaged friction coefficient is constant. In Ref. 1, direct methods were employed and the analysis was confined to the class of bodies whose longitudinal contour is a power law and whose transversal contour is semielliptical or triangular. In Ref. 2, the indirect methods of the calculus of variations were used and the longitudinal and transversal contours were optimized simultaneously. Concerning the longitudinal contour, it was shown that the optimum solution is conical and its thickness ratio is such that the friction drag is one-third of the total drag. Concerning the transversal contour, it was shown that the optimum solution is triangular with or without a keel, depending on whether the cross-sectional elongation ratio is smaller or larger than the critical value $\alpha = 4.85$.

Since Refs. 1 and 2 were limited to flat-top configurations, it is the purpose of this report to extend the investigation to more general lifting configurations, that is, configurations which are not necessarily flat-topped. The following hypotheses are employed: (a) a plane of symmetry exists between the left-hand and right-hand sides of the body; (b) the base plane is perpendicular to the plane of symmetry; (c) the body is homothetic, in the sense that each cross section is geometrically similar to and has the same orientation as the base cross section; (d) the body is longitudinally slender, that is, the square of the slope of any meridian contour is small with respect to one; (e) the free-stream velocity is contained in the plane of symmetry and is perpendicular to the base plane; (f) the pressure distribution is modified Newtonian, that is, the pressure coefficient is

proportional to the cosine squared of the angle formed by the free-stream velocity and the normal to each surface element; (g) the surface-averaged skin-friction coefficient is constant; (h) the base drag coefficient is zero; and (i) the contribution of the tangential forces to the lift is negligible with respect to the contribution of the normal forces.

2. LIFT-TO-DRAG RATIO

Consider two coordinate systems (Fig. 1): A Cartesian coordinate system Oxyz and a cylindrical coordinate system Oxrθ. For the Cartesian coordinate system, the origin O is the apex of the body; the x-axis is parallel to the free-stream velocity and positive toward the base; the z-axis is contained in the plane of symmetry, perpendicular to the x-axis, and positive downward; and the y-axis is such that the xyz-system is right-handed. For the cylindrical coordinate system, r is the distance of any point from the x-axis, and θ measures the angular position of the vector $\vec{r}$ with respect to the xy-plane.

In the cylindrical coordinate system, the geometry of an arbitrary body can be expressed in the form

$$r = r(x, \theta) \tag{1}$$

Therefore, if all the hypotheses of the introduction are employed, except for hypothesis (c), the drag D and the lift L per unit free-stream dynamic pressure q can be written as (Ref. 1)

$$\begin{aligned} D/q &= \int_0^{\ell} \int_{-\pi/2}^{\pi/2} \left[4nr^3 r_x^3/(r^2 + r_\theta^2) + 2C_f r/(r^2 + r_\theta^2)\right] dx d\theta \\ L/q &= \int_0^{\ell} \int_{-\pi/2}^{\pi/2} \left[4nr^2 r_x^2/(r^2 + r_\theta^2)\right] (r \sin\theta - r_\theta \cos\theta)\, dx d\theta \end{aligned} \tag{2}$$

where ℓ denotes the length of the body, C_f the surface-averaged skin-friction coefficient, and n a factor modifying the Newtonian pressure law[4].

---

[4] Under the slender-body approximation, the pressure coefficient employed in Eq. (2) is given by $C_p = 2nr^2 r_x^2/(r^2 + r_\theta^2)$.

If the body is homothetic, Eq. (1) takes the particular form

$$r = \ell\tau A(\xi) B(\theta) \tag{3}$$

where

$$\tau = h/\ell \tag{4}$$

is the thickness ratio, the ratio of the overall height h of the base section to the length ℓ of the body. In Eq. (3), the symbol $\xi = x/\ell$ denotes a dimensionless abscissa and $A(\xi)$ is a function describing the longitudinal contour such that

$$A(0) = 0 \quad , \quad A(1) = 1 \tag{5}$$

Also, the symbol $B(\theta)$ denotes a function describing the transversal contour, namely, the radius at any point of the base contour $r(\ell, \theta)$ normalized in terms of the overall height h. Substituting Eq. (3) into Eqs. (2) and defining the derivatives

$$\dot{A} = dA/d\xi \quad , \quad \dot{B} = dB/d\theta \tag{6}$$

we obtain the following relationships for the drag and the lift of a homothetic body:

$$D/q\ell^2 = 4n\tau^4 I_1 J_1 + 2C_f \tau I_2 J_2 \quad , \quad L/q\ell^2 = 4n\tau^3 I_3 J_3 \tag{7}$$

where I_1 , I_2 , I_3 denote the following integrals depending on the longitudinal contour:

$$I_1 = \int_0^1 A\dot{A}^3 d\xi \quad , \quad I_2 = \int_0^1 A d\xi \quad , \quad I_3 = \int_0^1 A\dot{A}^2 d\xi \tag{8}$$

and J_1 , J_2 , J_3 denote the following integrals depending on the transversal contour:

$$J_1 = \int_{-\pi/2}^{\pi/2} [B^6/(B^2 + \dot{B}^2)]d\theta$$

$$J_2 = \int_{-\pi/2}^{\pi/2} \sqrt{(B^2 + \dot{B}^2)}\, d\theta \tag{9}$$

$$J_3 = \int_{-\pi/2}^{\pi/2} [B^4/(B^2 + \dot{B}^2)]\ (B \sin\theta - \dot{B} \cos\theta)d\theta$$

From the previous discussion, it appears that--if the length ℓ, the thickness ratio τ, the longitudinal contour $A(\xi)$, and the transversal contour $B(\theta)$are given--the drag and the lift can be evaluated using Eqs. (7) through (9). Once these quantities are known, one can determine the aerodynamic efficiency or lift-to-drag ratio

$$E = L/D \tag{10}$$

which, in the light of Eqs. (7), can be written as

$$E = 2n\tau^2 I_3 J_3/(2n\tau^3 I_1 J_1 + C_f I_2 J_2) \tag{11}$$

3. OPTIMUM THICKNESS RATIO

We now suppose that the longitudinal contour $A(\xi)$ and the transversal contour $B(\theta)$ are arbitrarily prescribed, which means that the integrals I_1 , I_2 , I_3 and J_1 , J_2 , J_3 are known a priori. Then, assuming that the length ℓ is given and the surface-averaged skin-friction coefficient C_f has a value known a priori, we study the effect of the thickness ratio on the lift-to-drag ratio (11). Evidently, the lift-to-drag ratio is an extremum when the thickness ratio satisfies the relationship

$$E_\tau = 0 \tag{12}$$

whose explicit form

$$\tau\sqrt[3]{(n/C_f)} = \sqrt[3]{[(I_2/I_1)(J_2/J_1)]} \tag{13}$$

means that the skin-friction drag is one-third of the total drag. The associated maximum lift-to-drag ratio is given by

$$E\sqrt[3]{(C_f/n)} = (2/3)\sqrt[3]{(IJ)} \tag{14}$$

where the symbols I and J denote the following products of powers of integrals:

$$I = I_3^3/I_1^2 I_2 \quad , \quad J = J_3^3/J_1^2 J_2 \tag{15}$$

Clearly, the lift-to-drag ratio (14) depends on the longitudinal contour through the expression (15-1) and on the transversal contour through the expression (15-2). In turn, this leads to the separate optimization problems considered in Sections 4 and 5.

4. OPTIMUM LONGITUDINAL CONTOUR

Next, we consider bodies optimized with respect to the thickness ratio τ, assume that the transversal contour $B(\theta)$ is arbitrarily prescribed, and study the effect of the longitudinal contour $A(\xi)$ on the lift-to-drag ratio (14). Since the lift-to-drag ratio depends on the longitudinal contour through the expression (15-1), we formulate the following problem: "In the class of functions $A(\xi)$ which satisfy the end conditions (5), find that particular function which extremizes the functional (15-1), where the integrals I_1 , I_2 , I_3 are defined by Eqs. (8)."

The functional (15-1) is a product of powers of integrals whose end points are fixed and is governed by the theory set forth in Ref. 3. In this reference, it is shown that the previous problem is equivalent to that of extremizing the integral

$$\tilde{I} = \int_0^1 F(A, \dot{A}, \lambda_1, \lambda_2)\, d\xi \tag{16}$$

where the fundamental function is defined as

$$F = A(\dot{A}^2 - \lambda_1 \dot{A}^3 - \lambda_2) \tag{17}$$

and the undetermined, constant Lagrange multipliers are given by

$$\lambda_1 = 2I_3/3I_1 \quad , \quad \lambda_2 = I_3/3I_2 \tag{18}$$

Since the fundamental function does not contain the independent variable explicitly, standard methods of the calculus of variations show that the Euler equation

$$dF_{\dot{A}}/d\xi - F_A = 0 \tag{19}$$

admits the following first integral (see, for instance, Chapter 1 of Ref. 4):

$$F - \dot{A}F_{\dot{A}} = C \tag{20}$$

whose explicit form is

$$A(2\lambda_1\dot{A}^3 - \dot{A}^2 - \lambda_2) = C \tag{21}$$

Upon integrating Eq. (21) over the range 0, 1 and accounting for the definitions (8), we obtain the relationship

$$2\lambda_1 I_1 - I_3 - \lambda_2 I_2 = C \tag{22}$$

which is consistent with Eqs. (18) providing the integration constant has the value

$$C = 0 \tag{23}$$

Consequently, the differential equation of the extremal arc (21) becomes

$$2\lambda_1\dot{A}^3 - \dot{A}^2 - \lambda_2 = 0 \tag{24}$$

and implies that

$$\dot{A} = C_1 \tag{25}$$

where C_1 is a constant. Upon integrating this differential equation, we obtain the relationship

$$A = C_1\xi + C_2 \tag{26}$$

where, because of the end conditions (5), the constants take the values

$$C_1 = 1 \quad , \quad C_2 = 0 \tag{27}$$

In conclusion, the optimum longitudinal contour is described by

$$A = \xi \tag{28}$$

and, therefore, is conical. For this cone, the integrals (8) take the values

$$I_1 = I_2 = I_3 = 1/2 \tag{29}$$

and the Lagrange multipliers (18) are given by

$$\lambda_1 = 2/3 \quad , \quad \lambda_2 = 1/3 \tag{30}$$

Finally, the optimum thickness ratio (13) and the maximum lift-to-drag ratio (14) become

$$\tau\sqrt[3]{(n/C_f)} = \sqrt[3]{(J_2/J_1)} \quad , \quad E\sqrt[3]{(C_f/n)} = (2/3)\sqrt[3]{J} \tag{31}$$

5. TRANSVERSAL CONTOUR

In this section, we consider configurations optimized with respect to the thickness ratio τ and the longitudinal contour $A(\xi)$: these are conical configurations whose thickness ratio is such that the skin-friction drag is one-third of the total drag. Then, we study the effect of the transversal contour $B(\theta)$ on the optimum thickness ratio (31-1) and the associated lift-to-drag ratio (31-2).

In analogy with Section 4, one can formulate a variational problem, that of finding the function $B(\theta)$ which maximizes the lift-to-drag ratio (31-2) for given geometric constraints imposed on the cross section. For instance, the cross section may be required to be inscribed in a rectangular box of elongation ratio

$$\alpha = w/h \tag{32}$$

where w is the semiwidth and h the overall height. Since the lift-to-drag ratio (31-2) depends on the transversal contour through the expression (15-2), the previous problem consists of maximizing the product of powers of integrals (15-2), with the integrals J_1 , J_2 , J_3 being defined by Eqs. (9). This problem is considerably complicated and, hence, we postpone its solution to a subsequent report. Here, we present some introductory engineering considerations. For the sake of clarity, we divide the discussion into three cases depending on whether the projection of the apex of the conical body on the base section is located on, above, or below the maximum width line.

6. APEX ON THE MAXIMUM WIDTH LINE

Consider a conical body whose apex is located on the maximum width line and assume that the cross-sectional area is distributed partly above and partly below this line (Fig. 2). Then, compare the body under consideration (subscript a) with a flat-top body obtained from the former by eliminating all the area above the maximum width line (subscript b). Inspection of the dimensionless integrals (9) shows that the following inequalities hold:

$$J_{1a} > J_{1b} \quad , \quad J_{2a} > J_{2b} \quad , \quad J_{3a} < J_{3b} \tag{33}$$

with the consequence that

$$J_a < J_b \tag{34}$$

and that

$$E_a < E_b \tag{35}$$

Therefore, among all the bodies whose cross section has a given lower contour $B(\theta)$, the body (b) exhibits the highest lift-to-drag ratio.

6.1. One-Parameter Family. Here, we consider a one-parameter family of transversal contours (b) having the form

$$B = B(\theta, \alpha) \tag{36}$$

and observe that, for this family,

$$J_1 = J_1(\alpha) \quad , \quad J_2 = J_2(\alpha) \quad , \quad J_3 = J_3(\alpha) \tag{37}$$

Therefore, the optimum thickness ratio (31-1) and the maximum lift-to-drag ratio (31-2) are functions of the form

$$\tau\sqrt[3]{(n/C_f)} = f_1(\alpha) \quad , \quad E\sqrt[3]{(C_f/n)} = f_2(\alpha) \tag{38}$$

They are plotted in Figs. 4 and 5 for flat-top bodies whose cross sections are triangular, semielliptical, or rectangular (Fig. 3). For each given cross-sectional shape, a value of the elongation ratio exists which yields the highest lift-to-drag ratio. This value is given in Table 1 together with the associated optimum thickness ratio and maximum lift-to-drag ratio.

Table 1

Cross section	α	$\tau\sqrt[3]{(n/C_f)}$	$E\sqrt[3]{(C_f/n)}$
Triangular	∞	1.260	0.529
Semielliptical	1.467	1.004	0.367
Rectangular	0.401	1.570	0.366

From Figs. 4 and 5, it appears that, for a given elongation ratio α, flat-top bodies of triangular cross section exhibit higher lift-to-drag ratios and require higher thickness ratios than flat-top bodies of semielliptical or rectangular cross section.

The conclusions of this section are qualitatively consistent with the wind-tunnel tests reported by Whitehead in Ref. 5. Whitehead investigated conical configurations

having given length and volume and found that, for $\alpha = 1$ and $\alpha = 1.5$, the flat-top triangle is aerodynamically superior to the flat-top semiellipse and the rectangle. However, the relative changes in the lift-to-drag ratios of the configurations analyzed by Whitehead were found to be smaller than those predicted here; this is logical since the present work deals with unconstrained configurations while Ref. 5 dealt with constrained configurations (given length and volume).

6.2. Two-Parameter Family. Here, we consider a two-parameter family of transversal contours (b) having the form

$$B = B(\theta, \alpha, \beta) \tag{39}$$

and observe that, for this family,

$$J_1 = J_1(\alpha, \beta) \quad , \quad J_2 = J_2(\alpha, \beta) \quad , \quad J_3 = J_3(\alpha, \beta) \tag{40}$$

Therefore, the optimum thickness ratio (31-1) and the maximum lift-to-drag ratio (31-2) are functions of the form

$$\tau\sqrt[3]{(n/C_f)} = f_1(\alpha, \beta) \quad , \quad E\sqrt[3]{(C_f/n)} = f_2(\alpha, \beta) \tag{41}$$

They are plotted in Figs. 7 through 12 for flat-top bodies whose cross sections are trapezoidal, bitrapezoidal, or triangular with a keel. The parameter β, defined in Fig. 6, is such that these cross sections degenerate into a triangle for $\beta = 0$.

As Figs. 8 and 10 indicate, for each given elongation ratio α, increasing values of β correspond to decreasing values of the lift-to-drag ratio of the trapezoid and the bitrapezoid. Therefore, these cross sections are aerodynamically inferior to the pure triangle. For the triangle with a keel (Fig. 12), the lift-to-drag ratio decreases

monotonically with θ as long as $\alpha \geq 4.85$; for $\alpha \leq 4.85$, the lift-to-drag ratio exhibits a maximum when θ attains the particular value given in Fig. 13. The corresponding optimum thickness ratio and maximum lift-to-drag ratio are presented in Figs. 14 and 15. Consequently, the flat-top triangle with a keel is aerodynamically inferior to the pure triangle for $\alpha \geq 4.85$, while the converse is true for $\alpha \leq 4.85$. Incidentally, it has been shown in Ref. 2 that, among the cross sections of type (b), the pure triangle is the variational solution for $\alpha \geq 4.85$ and the triangle with a keel is the variational solution for $\alpha \leq 4.85$, as long as the values of θ are those given in Fig. 13.

7. APEX ABOVE THE MAXIMUM WIDTH LINE

Consider a conical body whose apex is located above the maximum width line and assume that the cross-sectional area is distributed partly above and partly below the lines joining the apex with the maximum width points (Fig. 16). Then, compare the body under consideration (subscript a) with a body obtained from the former by eliminating all the area above these lines (subscript b). Inspection of the dimensionless integrals (9) shows that Ineqs. (33) hold, with the consequence that Ineqs. (34) and (35) also hold. Therefore, among all the bodies whose cross section has a given lower contour $B(\theta)$, the body (b) exhibits the highest lift-to-drag ratio.

7.1. One-Parameter Family. Here, we consider a one-parameter family of transversal contours (b) having the form (36) and observe that, for this family, the functional relations (37) and (38) hold. The latter relations are plotted in Figs. 18 and 19 for flat-bottom bodies having triangular cross section (Fig. 17). For comparison purposes, the data relevant to some one-parameter families of transversal contours of type (a) are also exhibited, namely, flat-bottom bodies having semielliptical or rectangular cross section (Figs. 17 through 19). For each given cross-sectional shape, a value of the elongation ratio exists which yields the highest lift-to-drag ratio. This value is given in Table 2 together with the associated optimum thickness ratio and maximum lift-to-drag ratio.

Table 2

Cross section	α	$\tau_\lambda^3/(n/C_f)$	$E_\lambda^3/(C_f/n)$
Triangular	∞	1.260	0.529
Semielliptical	0.548	1.444	0.411
Rectangular	0.401	1.570	0.366

From Figs. 18 and 19, it appears that, for a given elongation ratio α, flat-bottom bodies of triangular cross section exhibit higher lift-to-drag ratios and require higher thickness ratios than flat-bottom bodies of semielliptical or rectangular cross section, a result in agreement with the experiments by Whitehead (Ref. 5). Comparison of Figs. 5 and 19 shows that the flat-bottom triangle is aerodynamically superior to the flat-top triangle regardless of the elongation ratio α,[5] a result also in agreement with Whitehead's experiments (Ref. 5).

7.2. Two-Parameter Family. Here, we consider a two-parameter family of transversal contours (b) having the form (39) and observe that, for this family, the functional relations (40) and (41) hold. They are plotted in Figs. 21 through 26 for bodies whose cross sections are triangles with a keel, caret shapes, and diamond shapes. The parameter β, defined in Fig. 20, is such that these cross sections degenerate into a flat-bottom triangle for $\beta = 0$.

As Figs. 22 and 24 indicate, for each given elongation ratio α, increasing values of β correspond to decreasing values of the lift-to-drag ratio of the triangle with a keel and the caret shape. Therefore, these cross sections are aerodynamically inferior to the flat-bottom triangle. For the diamond shape (Fig. 26), the lift-to-drag ratio exhibits a maximum when β attains the particular value given in Fig. 27. The corresponding optimum thickness ratio and maximum lift-to-drag ratio are presented in Figs. 28 and 29. Consequently, for a given elongation ratio α, we see that the diamond shape is aerodynamically superior to the flat-bottom triangle. By comparing Figs. 15 and 29, we also see that the diamond shape is aerodynamically superior to the flat-top triangle and the triangle with a keel. The relative differences are negligible for winglike configurations

[5] However, the lift-to-drag ratios of the flat-bottom triangle and the flat-top triangle become identical for $\alpha \to \infty$, that is, winglike configurations.

$[\alpha >> 1]$ but substantial for bodylike configuration $[\alpha \equiv 0(1)]$. Indeed, it can be proved that, among the cross sections of type (b), the diamond shape is the variational solution.

8. APEX BELOW THE MAXIMUM WIDTH LINE

Consider a conical body whose apex is located below the maximum width line and assume that the cross-sectional area is distributed partly above and partly below the lines joining the apex with the maximum width points (Fig. 30). Then compare the body under consideration (subscript a) with a body obtained from the former by eliminating all the area above these lines (subscript b). Inspection of the dimensionless integrals (9) shows that, while Ineqs. (33-1) and (33-3) are satisfied, Ineq. (33-2) may or may not be satisfied depending on the characteristics of the shape (a). In this connection, let θ_o denote the angle at which maximum width occurs, an asterisk denote the upper contour of the configuration (a), and K denote the quantity

$$K = 8J^*_{1a}/J_{1a} + [J^*_{2a} - B(\theta_o)]/J_{2a} - 9J^*_{3a}/J_{3a} \tag{42}$$

Then, it can be shown that

$$E_b > E_a \qquad \text{if} \qquad K > 0 \tag{43}$$

and

$$E_b < E_a \qquad \text{if} \qquad K < 0 \tag{44}$$

While both situations are physically possible, that described by Ineq. (43) is more likely to occur in practice.

For the above reasons, an example has been developed for the inverted caret shape indicated in Fig. 31. Analytically, shapes of this type constitute a two-parameter family having the form (39), where the parameter β has been chosen so that the value $\beta = 0$

corresponds to a flat-top triangle. For this family, the functional equations (40) and (41) are valid, and Eqs. (41) are plotted in Figs. 32 and 33. As Fig. 33 shows, for a given elongation ratio α, the lift-to-drag ratio decreases monotonically with the parameter β. Therefore, the inverted caret shape is aerodynamically inferior to the flat-top triangle.

9. DISCUSSION AND CONCLUSIONS

In the previous sections, the optimization of the lift-to-drag ratio of a slender, homothetic body flying at hypersonic speeds is presented under the assumptions that the pressure distribution is modified Newtonian and the surface-averaged skin-friction coefficient is constant. It is shown that a value of the thickness ratio exists which maximizes the lift-to-drag ratio; this particular value is such that the skin-friction drag is one-third of the total drag. The subsequent optimization of the longitudinal contour is reduced to the extremization of the product of the powers of three integrals related to the lift, the pressure drag, and the skin-friction drag. In this connection, it is proved that a conical solution is the best.

While the variational investigation of the optimum transversal contour is postponed to a subsequent paper, the effect of the main geometric parameters of a cross section on the lift-to-drag ratio is systematically analyzed. Three cases are discussed depending on whether the projection of the apex of the conical body on the base section is located on, above, or below the maximum width line.

Apex on the maximum width line. For a given lower contour of the cross section, high lift-to-drag ratios can be achieved by eliminating all the area above the maximum width line, that is, by using flat-top configurations. Among these, the following are investigated in detail: triangle, semiellipse, rectangle, trapezoid, bitrapezoid, and triangle with a keel. It is shown that the pure triangle and the triangle with a keel are superior to the rest. Specifically, for a given elongation ratio α, the former is the best providing $\alpha \geq 4.85$ while the latter is the best providing $\alpha \leq 4.85$.

Apex above the maximum width line. For a given lower contour of the cross section, high lift-to-drag ratios can be achieved by eliminating all the area above the lines joining the apex with the maximum width points. Among these configurations, the following are investigated in detail: triangle, triangle with a keel, caret shape, and diamond shape. For a given elongation ratio α, it is shown that the diamond shape is the best. It is also shown that it is superior to any of the flat-top shapes.

Apex below the maximum width line. For this case, no general conclusion has yet been found and only one example is developed: that of an inverted caret shape. The aerodynamic characteristics of this shape are poor by comparison with the best shapes analyzed previously.

ACKNOWLEDGEMENT

The authors are indebted to Mr. Bernard Spencer, Jr., NASA-Langley Research Center, for stimulating discussions.

APPENDIX A. CROSS-SECTIONAL CHARACTERISTICS

In this appendix, we present the main characteristics of the cross sections considered in Sections 6 through 8. Since the upper contour of these cross sections is composed of straight lines connecting the apex with the maximum width points, the integrals (9) can be rewritten as[6]

$$J_1 = \int_{\theta_o}^{\pi/2} [B^6/(B^2 + \dot{B}^2)]\, d\theta$$

$$J_2 = B(\theta_o) + \int_{\theta_o}^{\pi/2} \sqrt{(B^2 + \dot{B}^2)}\, d\theta \tag{45}$$

$$J_3 = \int_{\theta_o}^{\pi/2} [B^4/(B^2 + \dot{B}^2)](B \sin\theta - \dot{B} \cos\theta)\, d\theta$$

where θ_o denote the angular position of the maximum width points.

A.1. Flat-Top Triangle, $\theta_o = 0$. The lower contour is represented by

$$B = \alpha/(\alpha \sin\theta + \cos\theta) \quad , \quad \theta_o \le \theta \le \pi/2 \tag{46}$$

and the integrals (45) have the values

$$J_1 = \alpha^3/(1+\alpha^2) \quad , \quad J_2 = \alpha + \sqrt{(1+\alpha^2)} \quad , \quad J_3 = \alpha^3/(1+\alpha^2) \tag{47}$$

The evaluation of the quantity (15-2) shows that this quantity is stationary for

$$3\dot{J}_3/J_3 - 2\dot{J}_1/J_1 - \dot{J}_2/J_2 = 0 \tag{48}$$

---

[6] An exception is the flat-bottom semiellipse.

where the dot sign denotes a derivative with respect to the elongation ratio α. The solution of this equation is

$$\alpha = \infty \tag{49}$$

meaning that, if the cross section is a flat-top triangle, a winglike configuration is desirable. The corresponding values of the thickness ratio and the lift-to-drag ratio are

$$\tau\sqrt[3]{(n/C_f)} = 1.260 \quad , \quad E\sqrt[3]{(C_f/n)} = 0.529 \tag{50}$$

As an example, for $C_f/n = 10^{-3}$, the optimum thickness ratio is $\tau = 0.126$ and the maximum lift-to-drag ratio is $E = 5.29$.

A.2. Flat-Top Semiellipse, $\theta_o = 0$. The lower contour is represented by

$$B = \alpha/\sqrt{(\alpha^2 \sin^2\theta + \cos^2\theta)} \quad , \quad \theta_o \le \theta \le \pi/2 \tag{51}$$

and the integrals (45) have the values

$$J_1 = \pi\alpha^2/2$$

$$J_2 = \alpha[1 + E(\pi/2 \, , \gamma/\alpha)] \tag{52}$$

$$J_3 = (\alpha^2/2\gamma) \log [(\alpha + \gamma)/(\alpha - \gamma)]$$

where $\gamma = \sqrt{(\alpha^2 - 1)}$ and where E denotes the complete elliptic integral of the second kind. The evaluation of the quantity (15-2) shows that a maximum occurs when Eq. (48) is satisfied. Its solution is

$$\alpha = 1.467 \tag{53}$$

and the corresponding optimum thickness ratio and maximum lift-to-drag ratio are

$$\tau\sqrt[3]{(n/C_f)} = 1.004 \quad , \quad E\sqrt[3]{(C_f/n)} = 0.367 \tag{54}$$

A.3. Rectangle, $\theta_o = 0$. The lower contour is represented by

$$\begin{aligned} B &= \alpha/\cos\theta \quad , \quad \theta_o \le \theta \le \arctan(1/\alpha) \\ B &= 1/\sin\theta \quad , \quad \arctan(1/\alpha) \le \theta \le \pi/2 \end{aligned} \tag{55}$$

and the integrals (45) have the values

$$J_1 = \alpha(1+\alpha^2) \quad , \quad J_2 = 1 + 2\alpha \quad , \quad J_3 = \alpha \tag{56}$$

The evaluation of the quantity (15-2) shows that this quantity is stationary when Eq. (48) is satisfied. Its solution is

$$\alpha = 0.401 \tag{57}$$

and the corresponding optimum thickness ratio and maximum lift-to-drag ratio are

$$\tau\sqrt[3]{(n/C_f)} = 1.570 \quad , \quad E\sqrt[3]{(C_f/n)} = 0.366 \tag{58}$$

A.4. Trapezoid, $\theta_o = 0$. The lower contour is represented by

$$\begin{aligned} B &= \alpha/[(\alpha - \theta)\sin\theta + \cos\theta] \quad , \quad \theta_o \le \theta \le \arctan(1/\theta) \\ B &= 1/\sin\theta \quad , \quad \arctan(1/\theta) \le \theta \le \pi/2 \end{aligned} \tag{59}$$

and the integrals (45) have the values

$$J_1 = \beta + \alpha^3/[1 + (\alpha - \beta)^2]$$

$$J_2 = \alpha + \beta + \sqrt{[1 + (\alpha - \beta)^2]} \tag{60}$$

$$J_3 = \beta + \alpha^2(\alpha - \beta)/[1 + (\alpha - \beta)^2]$$

For a given elongation ratio α, the quantity (15-2) decreases monotonically with the parameter β. Hence, this quantity has its highest value at

$$\beta = 0 \tag{61}$$

which means that a triangle is aerodynamically superior to the present configuration.

A.5. Bitrapezoid, $\theta_o = 0$. The lower contour is represented by

$$\begin{aligned} B &= \alpha/\cos\theta \quad , && \theta_o \le \theta \le \arctan(\beta/\alpha) \\ B &= \alpha/[\alpha\sin\theta + (1 - \beta)\cos\theta] \quad , && \arctan(\beta/\alpha) \le \theta \le \pi/2 \end{aligned} \tag{62}$$

and the integrals (45) have the values

$$J_1 = \beta\alpha^3 + \alpha^3/[\alpha^2 + (1 - \beta)^2]$$

$$J_2 = \alpha + \beta + \sqrt{[\alpha^2 + (1 - \beta)^2]} \tag{63}$$

$$J_3 = \alpha^3/[\alpha^2 + (1 - \beta)^2]$$

For a given elongation ratio α, the quantity (15-2) decreases monotonically with the

parameter β. Hence, this quantity has its highest value at

$$\beta = 0 \tag{64}$$

which means that a triangle is aerodynamically superior to the present configuration.

A.6. Flat-Top Triangle with a Keel, $\theta_o = 0$. The lower contour is represented by

$$\begin{aligned} B &= \alpha(1 - \beta)/[\alpha \sin\theta + (1 - \beta)\cos\theta] \quad , \quad \theta_o \le \theta \le \pi/2 \\ 1 - \beta &\le B \le 1 \quad , \quad \theta = \pi/2 \end{aligned} \tag{65}$$

and the integrals (45) have the values

$$\begin{aligned} J_1 &= \alpha^3(1 - \beta)^3/[\alpha^2 + (1 - \beta)^2] \\ J_2 &= \alpha + \beta + \sqrt{[\alpha^2 + (1 - \beta)^2]} \\ J_3 &= \alpha^3(1 - \beta)^2/[\alpha^2 + (1 - \beta)^2] \end{aligned} \tag{66}$$

For a given elongation ratio α, the quantity (15-2) has a maximum with respect to the parameter β providing Eq. (48) is satisfied, with the dot sign denoting a derivative with respect to β. After Eq. (48) is rewritten as

$$\alpha^2 - (1 - \beta)\{2\alpha + 3\beta - 1 + 3\sqrt{[\alpha^2 + (1 - \beta)^2]}\} = 0 \tag{67}$$

we see that nonnegative solutions for β occur in the range $\alpha \le 4.85$. Therefore, the flat-top triangle with a keel is aerodynamically superior to the pure triangle for $\alpha < 4.85$, while the converse holds for $\alpha > 4.85$.

A.7. Flat-Bottom Triangle, $\theta_o = \arctan(1/\alpha)$. The lower contour is represented by

$$B = 1/\sin\theta \quad , \quad \theta_o \le \theta \le \pi/2 \tag{68}$$

and the integrals (45) have the values

$$J_1 = \alpha \quad , \quad J_2 = \alpha + \sqrt{(1+\alpha^2)} \quad , \quad J_3 = \alpha \tag{69}$$

The quantity (15-2) is stationary when Eq. (48) is satisfied. The solution of this equation is

$$\alpha = \infty \tag{70}$$

meaning that, if the cross section is a flat-bottom triangle, a winglike configuration is desirable. The corresponding values of the thickness ratio and the lift-to-drag ratio are given by Eqs. (50).

A.8. Flat-Bottom Semiellipse. The upper and lower contours are represented by

$$\begin{aligned} B &= 2\alpha^2 \sin\theta/(\alpha^2\sin^2\theta + \cos^2\theta) \quad , \quad 0 \le \theta \le \arctan(1/\alpha) \\ B &= 1/\sin\theta \quad , \quad \arctan(1/\alpha) \le \theta \le \pi/2 \end{aligned} \tag{71}$$

and the integrals (9) have the values

$$\begin{aligned} J_1 &= \alpha - \alpha^3/\gamma^2 + \pi\alpha^2(\alpha+4)/2(\alpha+1) \\ &\quad + [\alpha^2(4-3\alpha^2)/2\gamma^3]\log[(\alpha+\gamma)/(\alpha-\gamma)] \\ J_2 &= 2\alpha + (\alpha-\gamma)\,F(\varphi, k) - (\alpha+\gamma)\,[1 - E(\varphi, k)] \\ J_3 &= \alpha - \alpha^3/\gamma^2 + \pi\alpha^2/(\alpha+1) \\ &\quad + [\alpha^2(2-\alpha^2)/2\gamma^3]\log[(\alpha+\gamma)/(\alpha-\gamma)] \end{aligned} \tag{72}$$

where $\gamma = \sqrt{(\alpha^2 - 1)}$. Here, F and E denote the incomplete elliptic integrals of the first and the second kind, whose argument φ and parameter k are given by

$$\varphi = \arctan(\alpha + \gamma)$$
$$k = 2\sqrt{(\alpha\gamma)}/(\alpha + \gamma) \tag{73}$$

The evaluation of the quantity (15-2) shows that a maximum occurs when Eq. (48) is satisfied. Its solution is

$$\alpha = 0.548 \tag{74}$$

and the corresponding optimum thickness ratio and maximum lift-to-drag ratio are

$$\tau \sqrt[3]{(n/C_f)} = 1.444 \quad , \quad E \sqrt[3]{(C_f/n)} = 0.411 \tag{75}$$

A.9. Flat-Bottom Triangle with a Keel, $\theta_o = \arctan[(1 - \beta)/\alpha]$. The lower contour is represented by

$$B = (1 - \beta)/\sin\theta \quad , \quad \theta_o \le \theta \le \pi/2$$
$$1 - \beta \le B \le 1 \quad , \quad \theta = \pi/2 \tag{76}$$

and the integrals (45) have the values

$$J_1 = \alpha(1 - \beta)^3$$
$$J_2 = \alpha + \beta + \sqrt{[\alpha^2 + (1 - \beta)^2]} \tag{77}$$
$$J_3 = \alpha(1 - \beta)^2$$

For a given elongation ratio α, the quantity (15-2) decreases monotonically with the parameter β. Hence, this quantity has its highest value at

$$\beta = 0 \tag{78}$$

which means that a flat-bottom triangle is aerodynamically superior to the present configuration.

A. 10. Caret Shape, $\theta_o = \arctan(1/\alpha)$. The lower contour is represented by

$$B = \alpha(1 - \beta)/(\alpha \sin\theta - \beta\cos\theta) \quad , \qquad \theta_o \le \theta \le \pi/2 \tag{79}$$

and the integrals (45) have the values

$$\begin{aligned} J_1 &= \alpha^3(1 - \beta)^3/(\alpha^2 + \beta^2) \\ J_2 &= \sqrt{(1 + \alpha^2)} + \sqrt{(\alpha^2 + \beta^2)} \\ J_3 &= \alpha^3(1 - \beta)^2/(\alpha^2 + \beta^2) \end{aligned} \tag{80}$$

For a given elongation ratio α, the quantity (15-2) decreases monotonically with the parameter β. Hence, this quantity has its highest value at

$$\beta = 0 \tag{81}$$

which means that a flat-bottom triangle is aerodynamically superior to the present configuration.

A.11. Diamond Shape, $\theta_o = \arctan[(1 - \beta)/\alpha]$. The lower contour is represented by

$$B = \alpha/(\alpha \sin\theta + \beta\cos\theta) \quad , \quad \theta_o \le \theta \le \pi/2 \tag{82}$$

and the integrals (45) have the values

$$J_1 = \alpha^3/(\alpha^2 + \beta^2)$$

$$J_2 = \sqrt{(\alpha^2 + \beta^2)} + \sqrt{[\alpha^2 + (1 - \beta)^2]} \tag{83}$$

$$J_3 = \alpha^3/(\alpha^2 + \beta^2)$$

For a given elongation ratio α, the quantity (15-2) has a maximum with respect to the parameter β providing Eq. (48) is satisfied, with the dot sign denoting a derivative with respect to β. After Eq. (48) is rewritten as

$$(\alpha^2 + \beta^2)\left[4\dot{\beta} - 3\beta - 3\sqrt{(\beta^2 + 8\beta)}\right] + 8\beta(2\beta - 1) = 0 \tag{84}$$

we see that the optimum diamond shape determined by Eq. (84) is aerodynamically superior to both the flat-top triangle ($\beta = 1$) and the flat-bottom triangle ($\beta = 0$) having the same value of α.

A.12. Inverted Caret Shape, $\theta_o = -\arctan(\beta/\alpha)$. The lower contour is represented by

$$B = \alpha(1 - \beta)/(\alpha \sin\theta + \cos\theta) \quad , \quad \theta_o \le \theta \le \pi/2 \tag{85}$$

and the integrals (45) have the values

$$J_1 = \alpha^3(1 - \beta)^3/(1 + \alpha^2)$$

$$J_2 = \sqrt{(1 + \alpha^2)} + \sqrt{(\alpha^2 + \beta^2)} \tag{86}$$

$$J_3 = \alpha^3(1 - \beta)^2/(1 + \alpha^2)$$

For a given elongation ratio α, the quantity (15-2) decreases monotonically with the parameter β. Hence, this quantity has its highest value at

$$\beta = 0 \tag{87}$$

which means that the flat-top triangle is aerodynamically superior to the present configuration.

REFERENCES

1. MIELE, A., Lift-to-Drag Ratios of Slender Bodies at Hypersonic Speeds, Journal of the Astronautical Sciences, Vol. 13, No. 1, 1966.

2. MIELE, A., HULL, D.G., and BROWN, S.L., Maximum Lift-to-Drag Ratio of a Slender, Flat-Top, Hypersonic Body, Astronautica Acta, Vol. 13, No. 2, 1967.

3. MIELE, A., On the Minimization of the Product of the Powers of Several Integrals, Journal of Optimization Theory and Applications, Vol. 1, No. 1, 1967.

4. MIELE, A., Editor, Theory of Optimum Aerodynamic Shapes, Academic Press, New York, 1965.

5. WHITEHEAD, A.H., Jr., Effect of Body Cross Section and Width-Height Ratio on Performance of Bodies and Delta-Wing-Body Combinations at Mach 6.9, NASA TN No. D-2886, 1966.

LIST OF CAPTIONS

Fig. 1 Coordinate system.

Fig. 2 Cross sections with the apex on the maximum width line.

Fig. 3 Particular cross sections.

Fig. 4 Optimum thickness ratio.

Fig. 5 Maximum lift-to-drag ratio.

Fig. 6 Particular cross sections.

Fig. 7 Optimum thickness ratio.

Fig. 8 Maximum lift-to-drag ratio.

Fig. 9 Optimum thickness ratio.

Fig. 10 Maximum lift-to-drag ratio.

Fig. 11 Optimum thickness ratio.

Fig. 12 Maximum lift-to-drag ratio.

Fig. 13 Optimum value of the parameter β.

Fig. 14 Optimum thickness ratio.

Fig. 15 Maximum lift-to-drag ratio.

Fig. 16 Cross sections with the apex above the maximum width line.

Fig. 17 Particular cross sections.

Fig. 18 Optimum thickness ratio.

Fig. 19 Maximum lift-to-drag ratio.

Fig. 20 Particular cross sections.

Fig. 21 Optimum thickness ratio.

Fig. 22 Maximum lift-to-drag ratio.

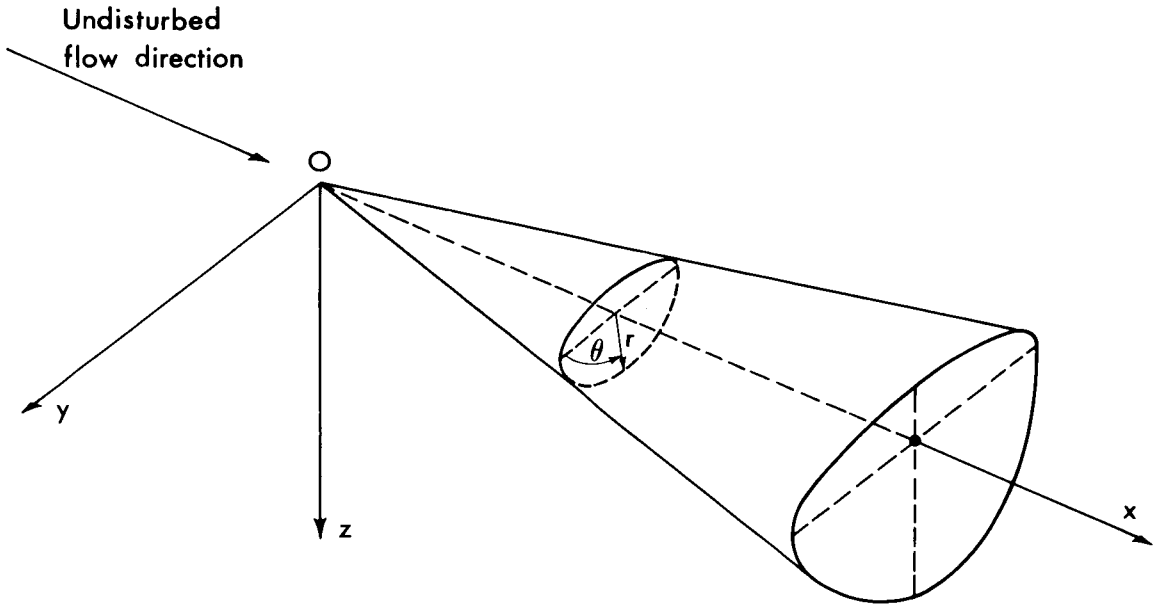

Fig. 1 Coordinate system.

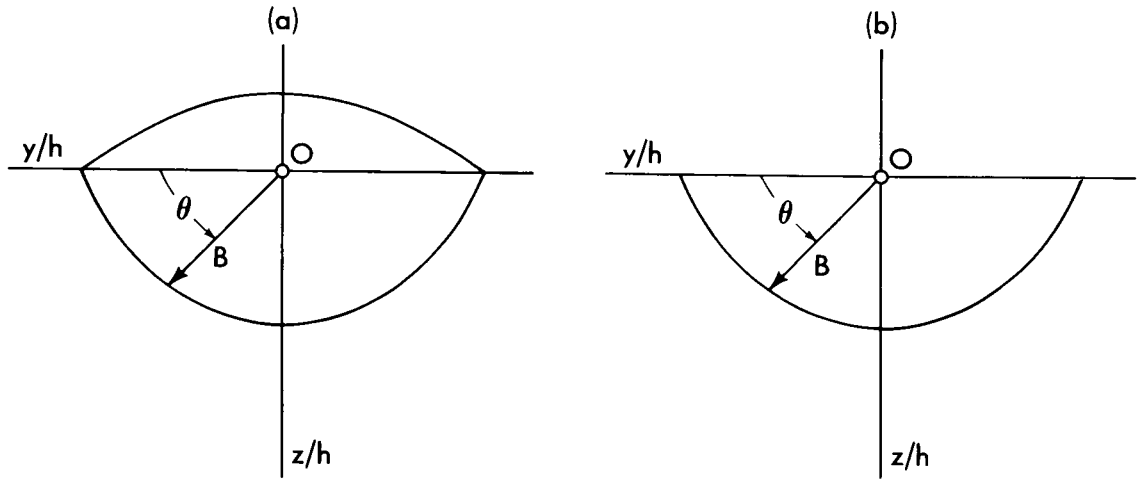

Fig. 2 Cross sections with the apex on the maximum width line.

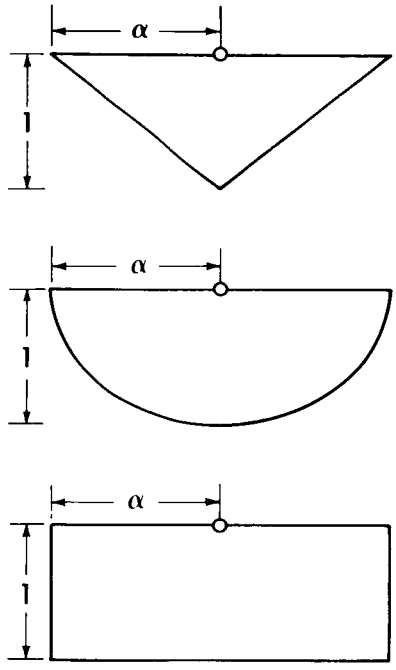

Fig. 3 Particular cross sections.

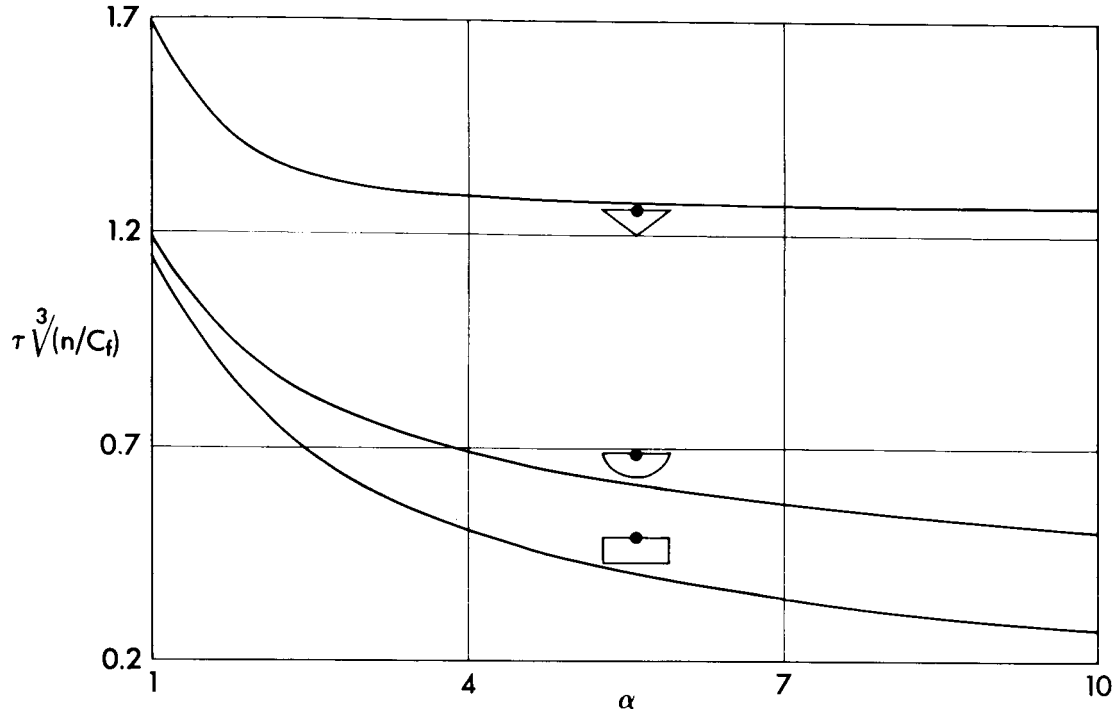

Fig. 4 Optimum thickness ratio.

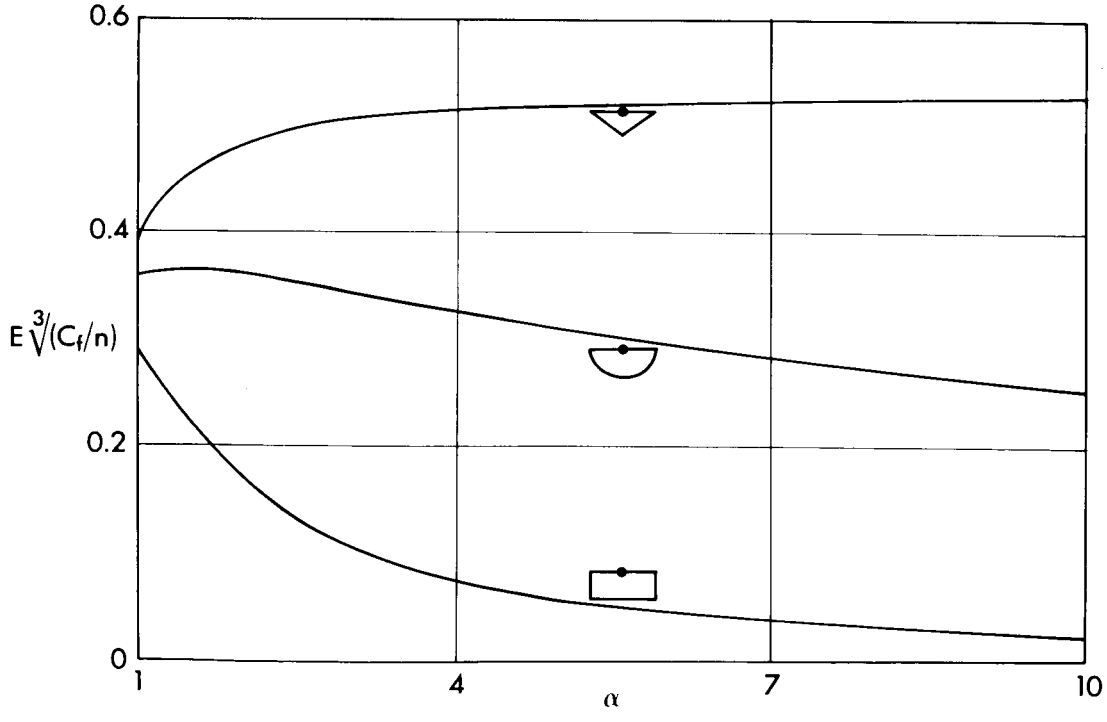

Fig. 5 Maximum lift-to-drag ratio.

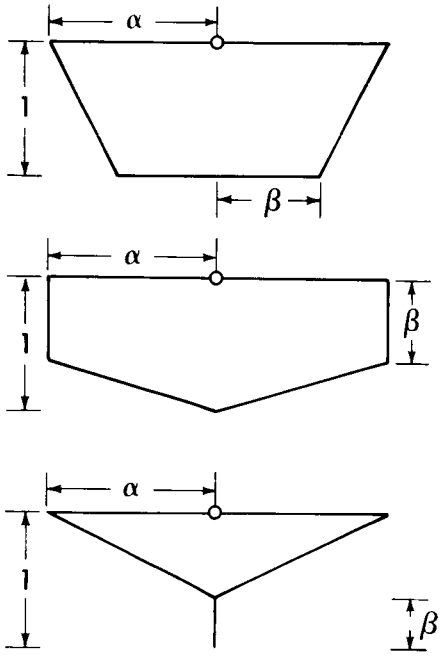

Fig. 6 Particular cross sections.

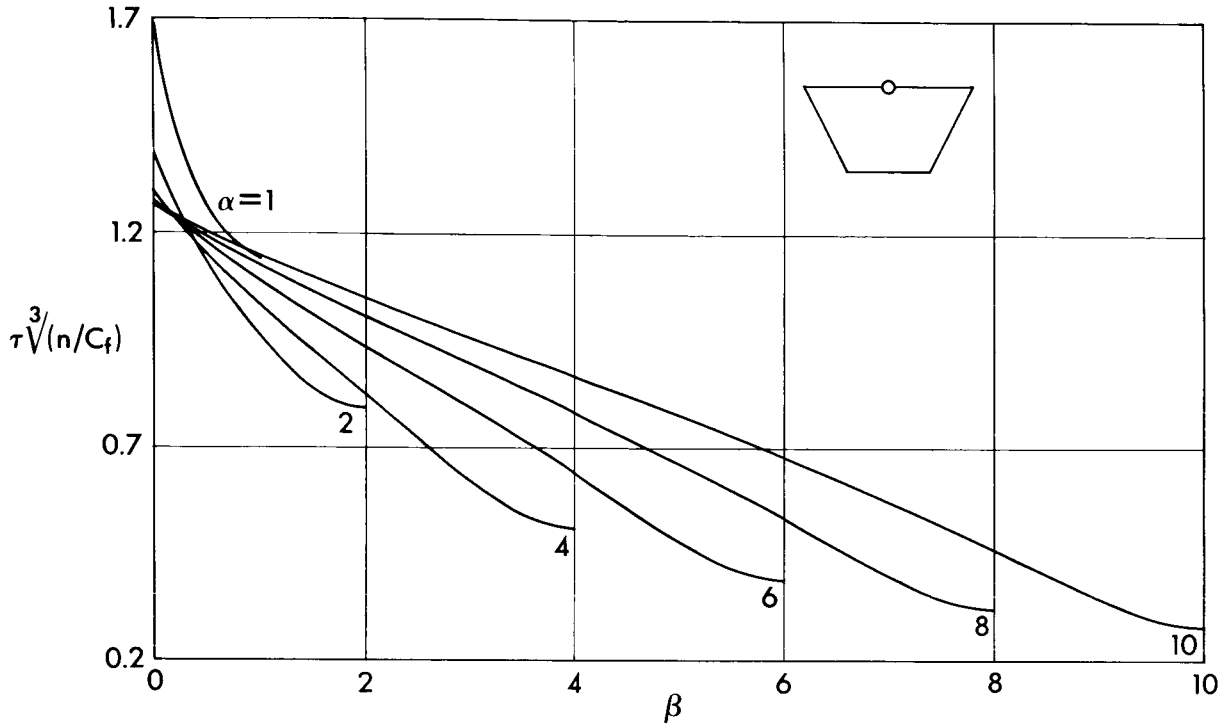

Fig. 7 Optimum thickness ratio.

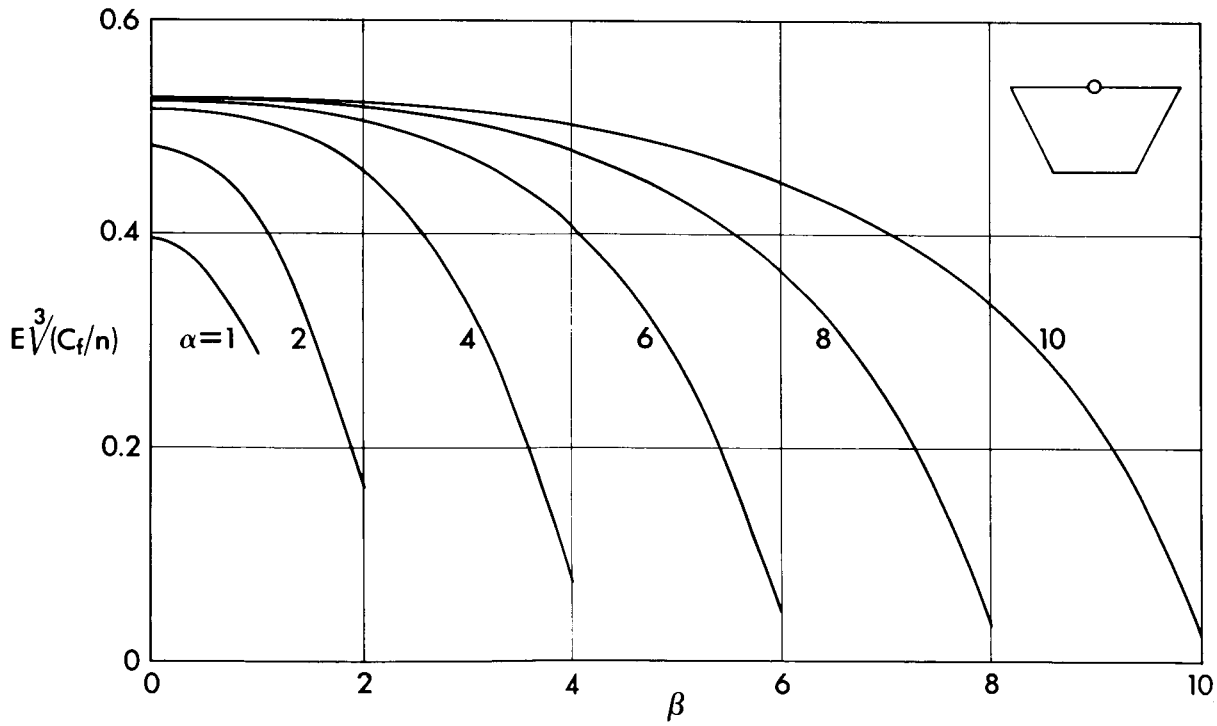

Fig. 8 Maximum lift-to-drag ratio.

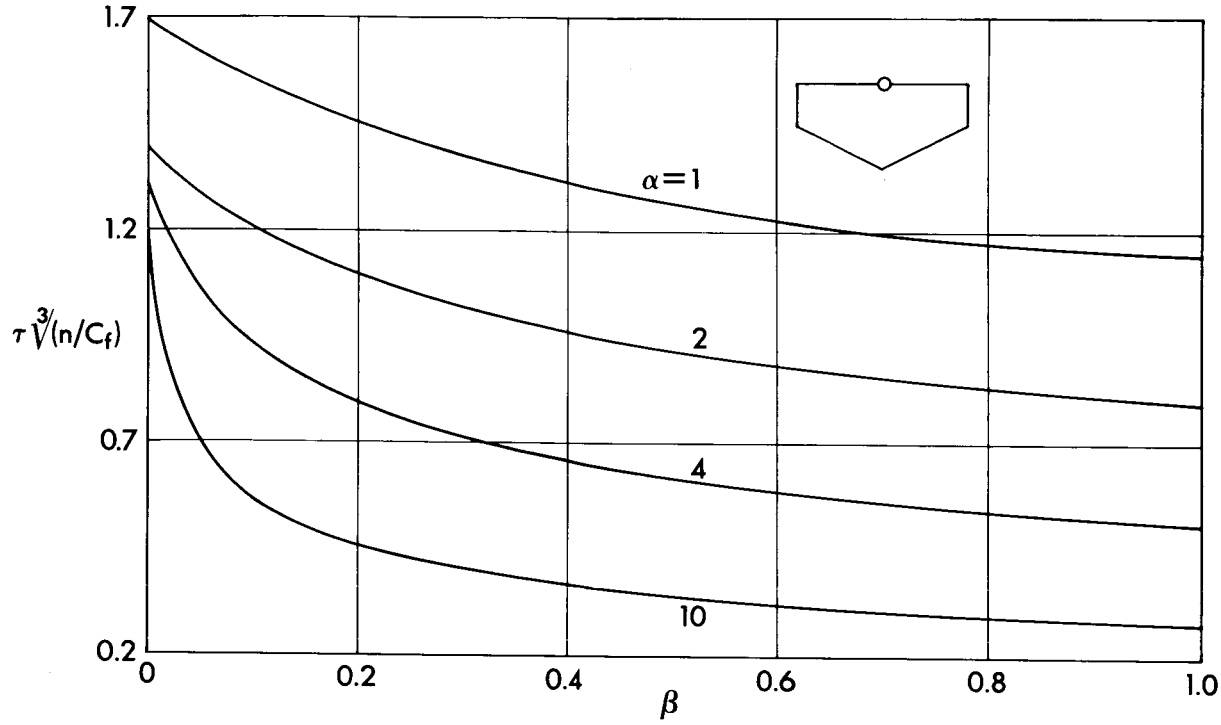

Fig. 9 Optimum thickness ratio.

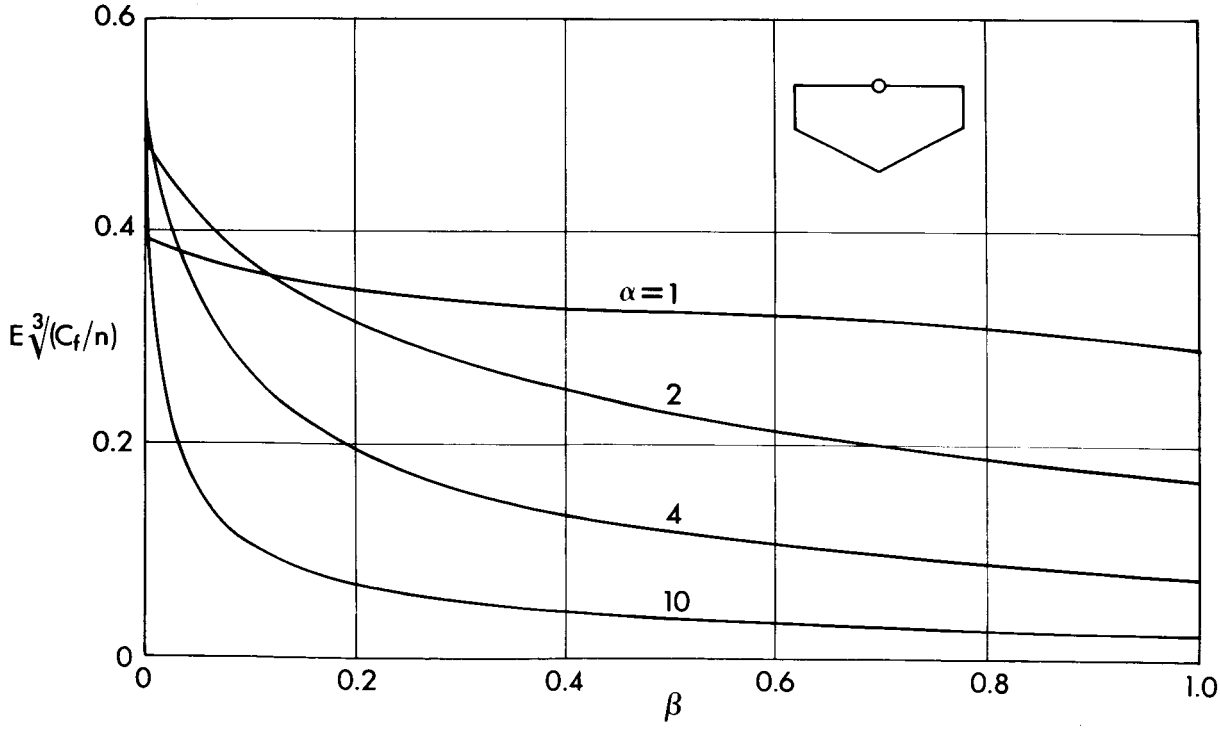

Fig. 10 Maximum lift-to-drag ratio.

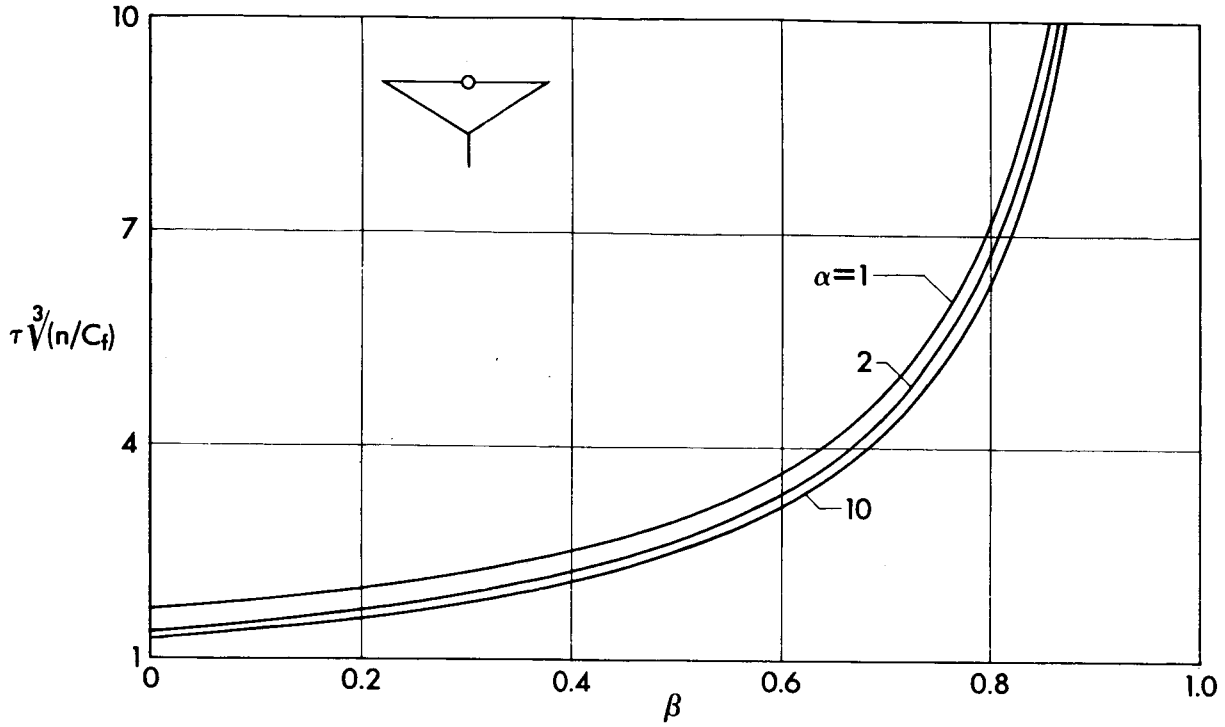

Fig. 11 Optimum thickness ratio.

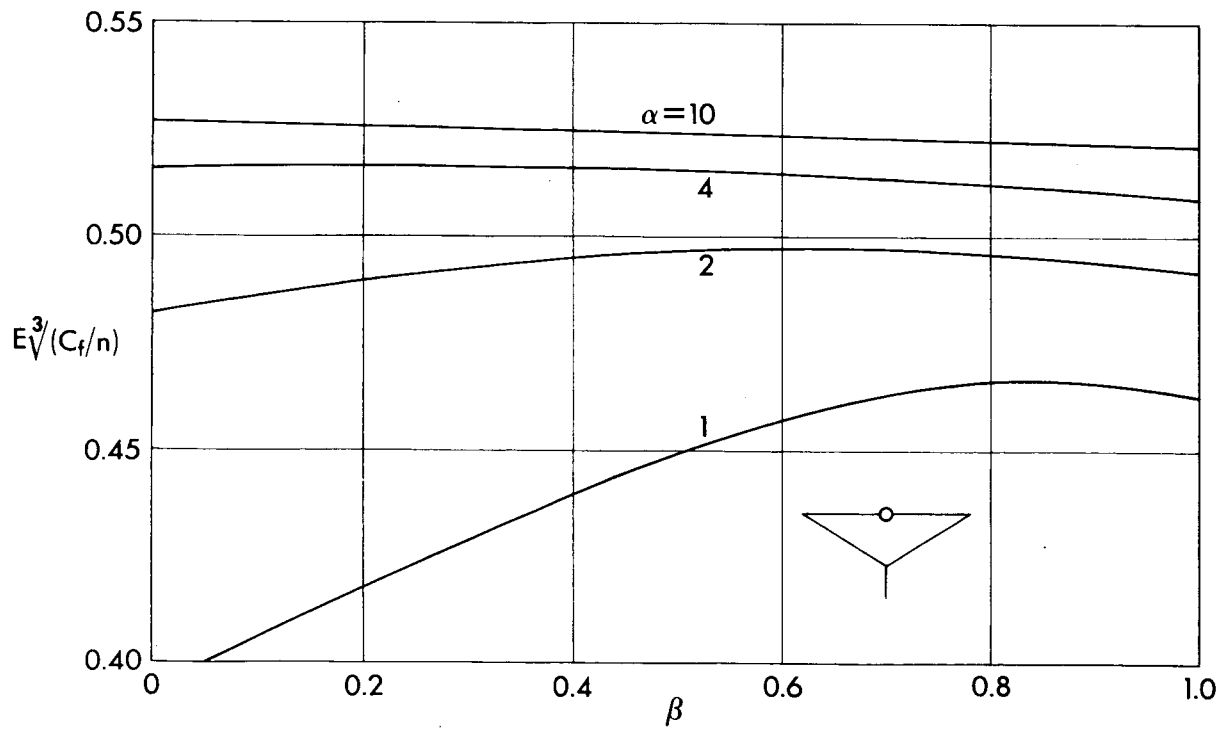

Fig. 12 Maximum lift-to-drag ratio.

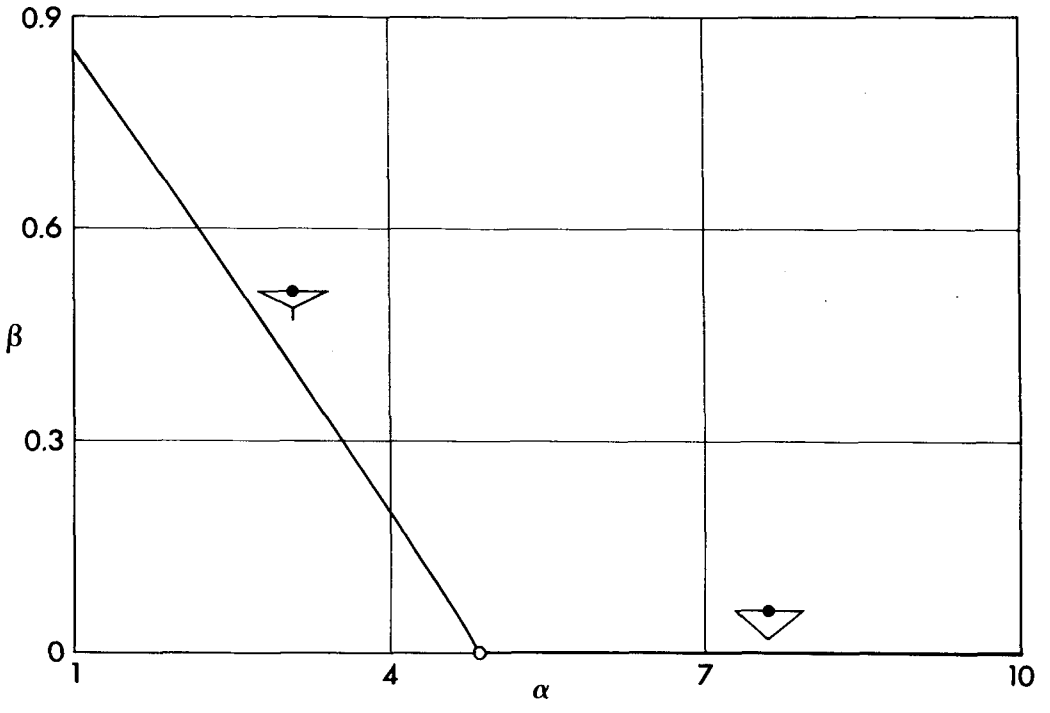

Fig. 13 Optimum value of the parameter θ.

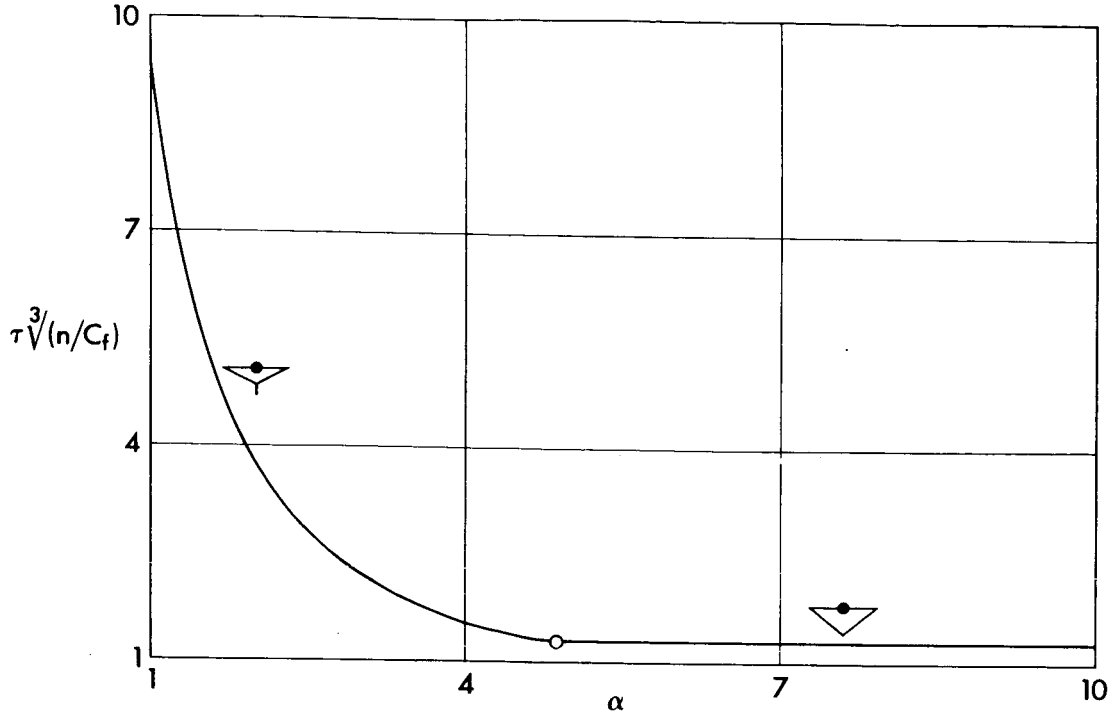

Fig. 14 Optimum thickness ratio.

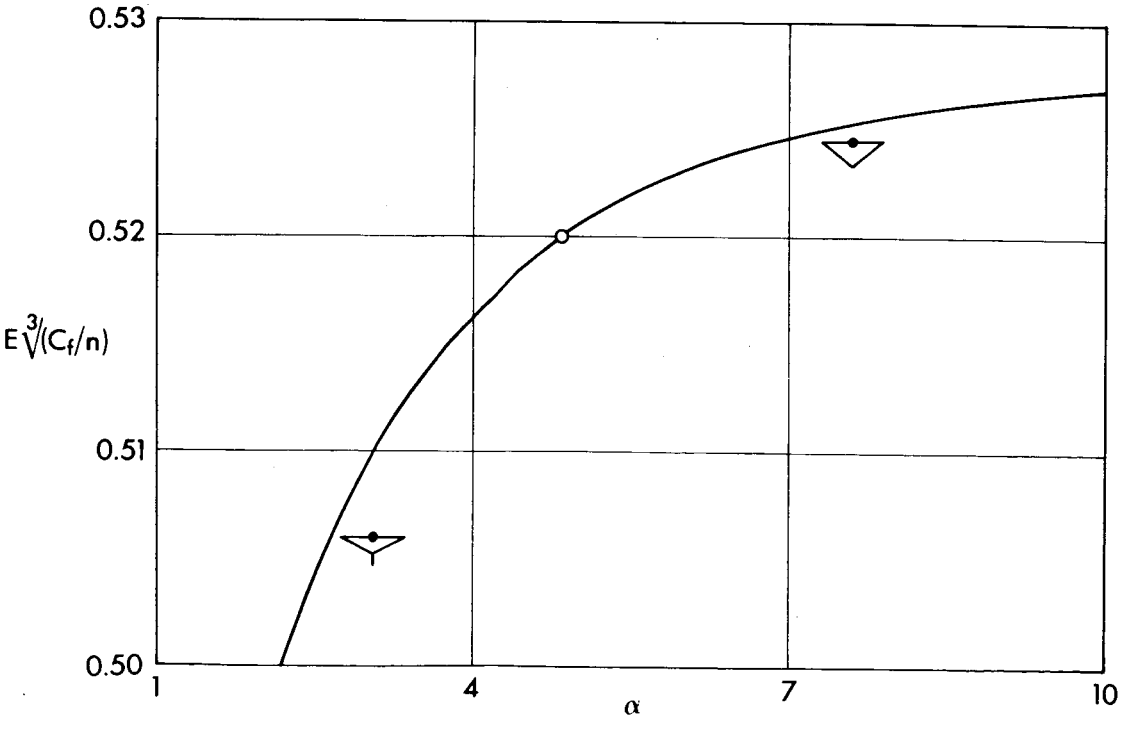

Fig. 15 Maximum lift-to-drag ratio.

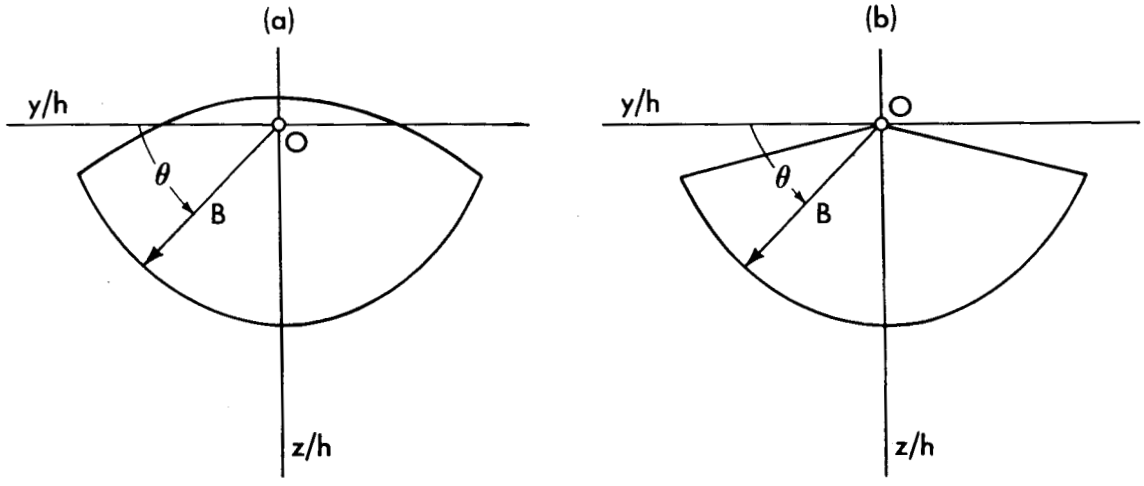

Fig. 16 Cross sections with the apex above the maximum width line.

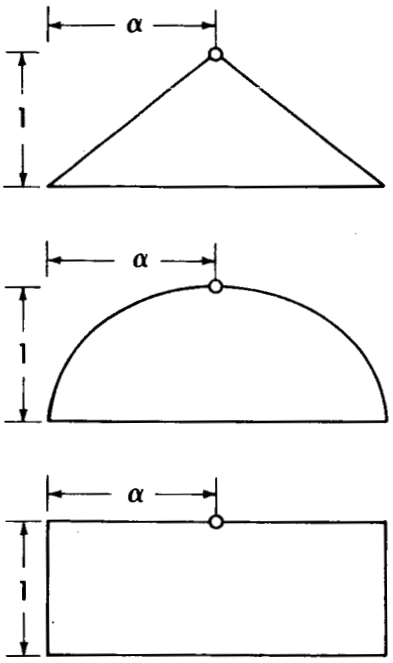

Fig. 17 Particular cross sections.

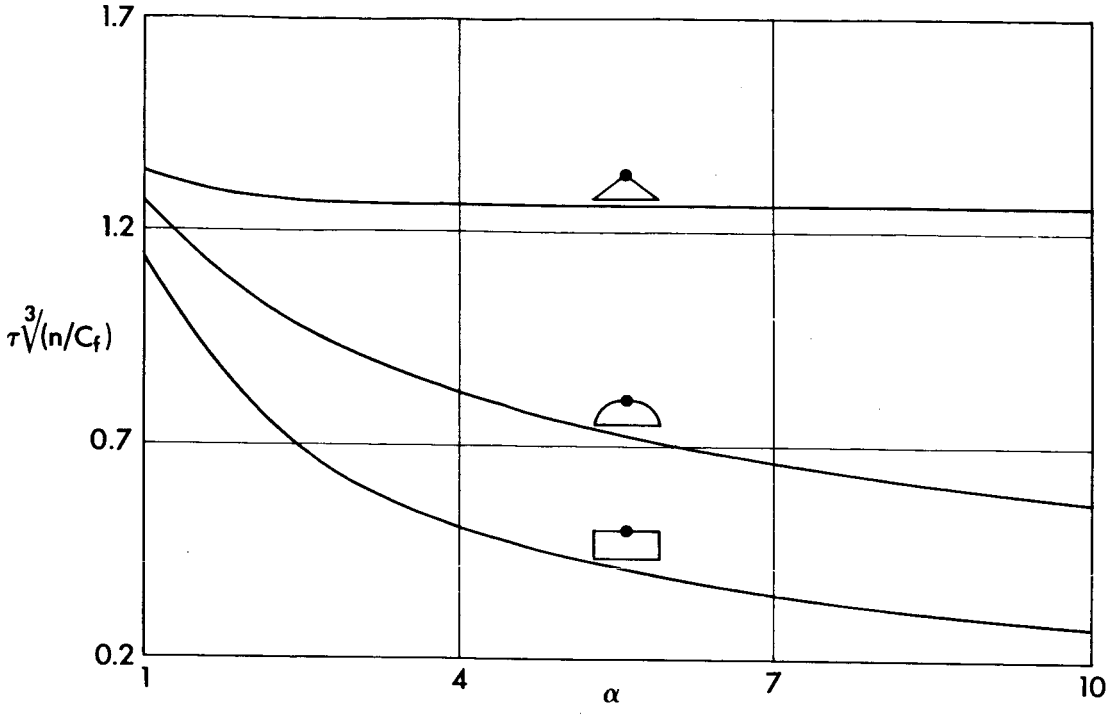

Fig. 18 Optimum thickness ratio.

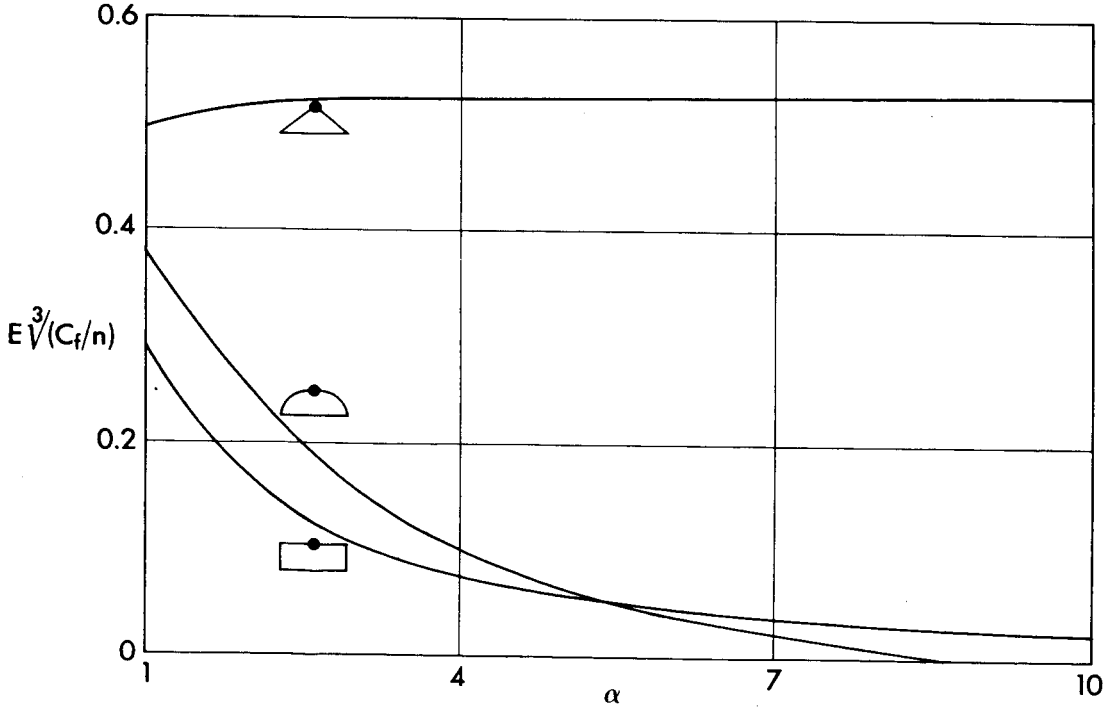

Fig. 19 Maximum lift-to-drag ratio.

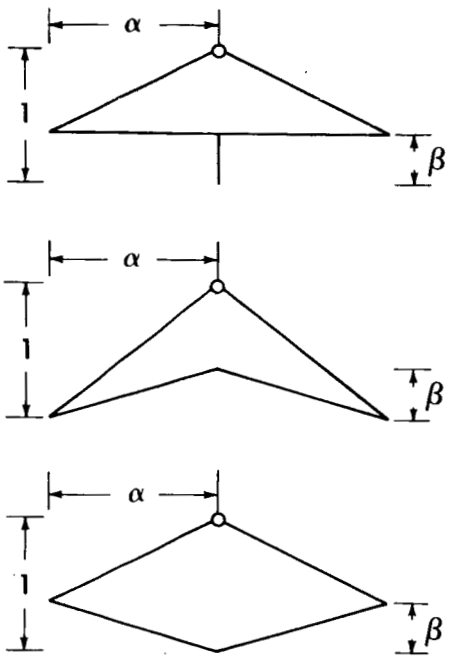

Fig. 20 Particular cross sections.

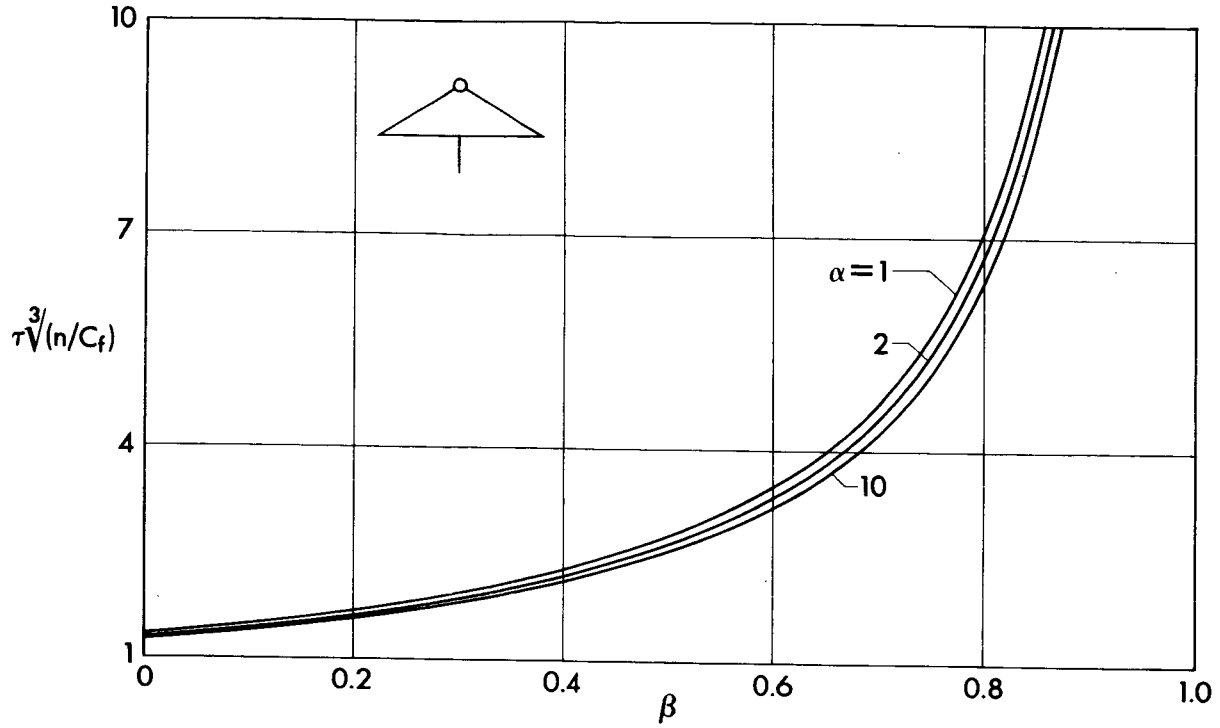

Fig. 21 Optimum thickness ratio.

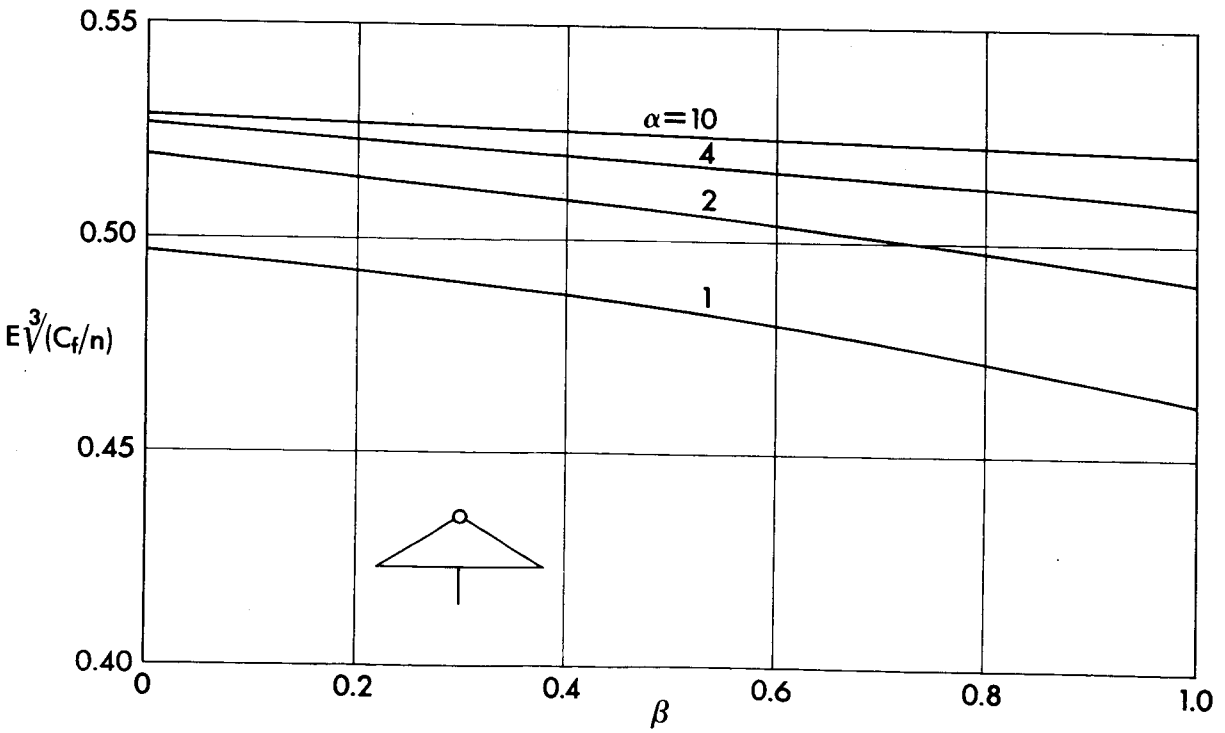

Fig. 22 Maximum lift-to-drag ratio.

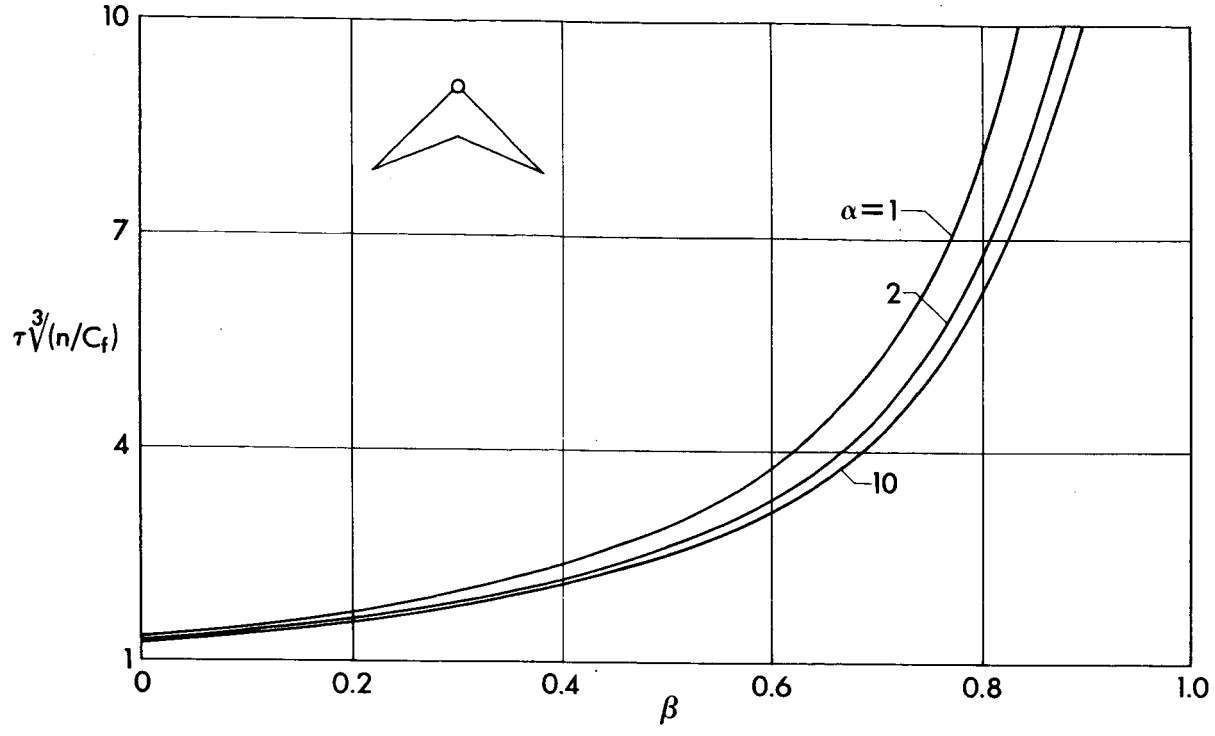

Fig. 23 Optimum thickness ratio.

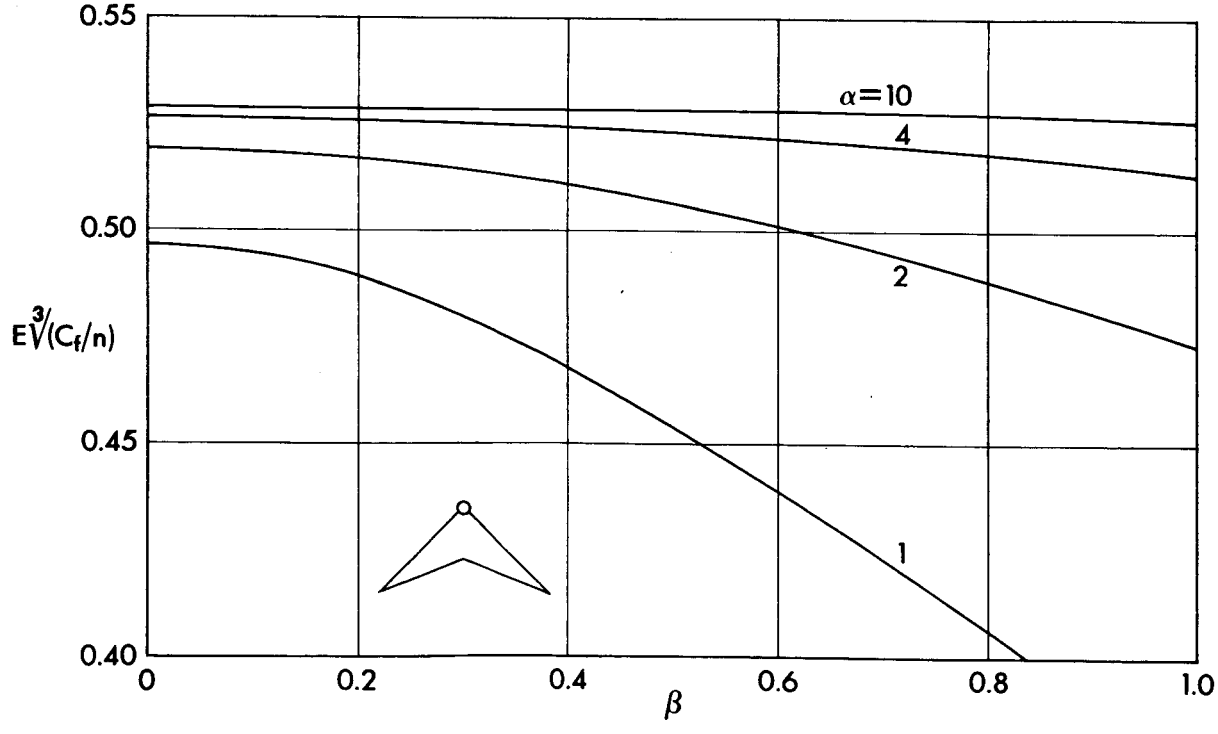

Fig. 24 Maximum lift-to-drag ratio.

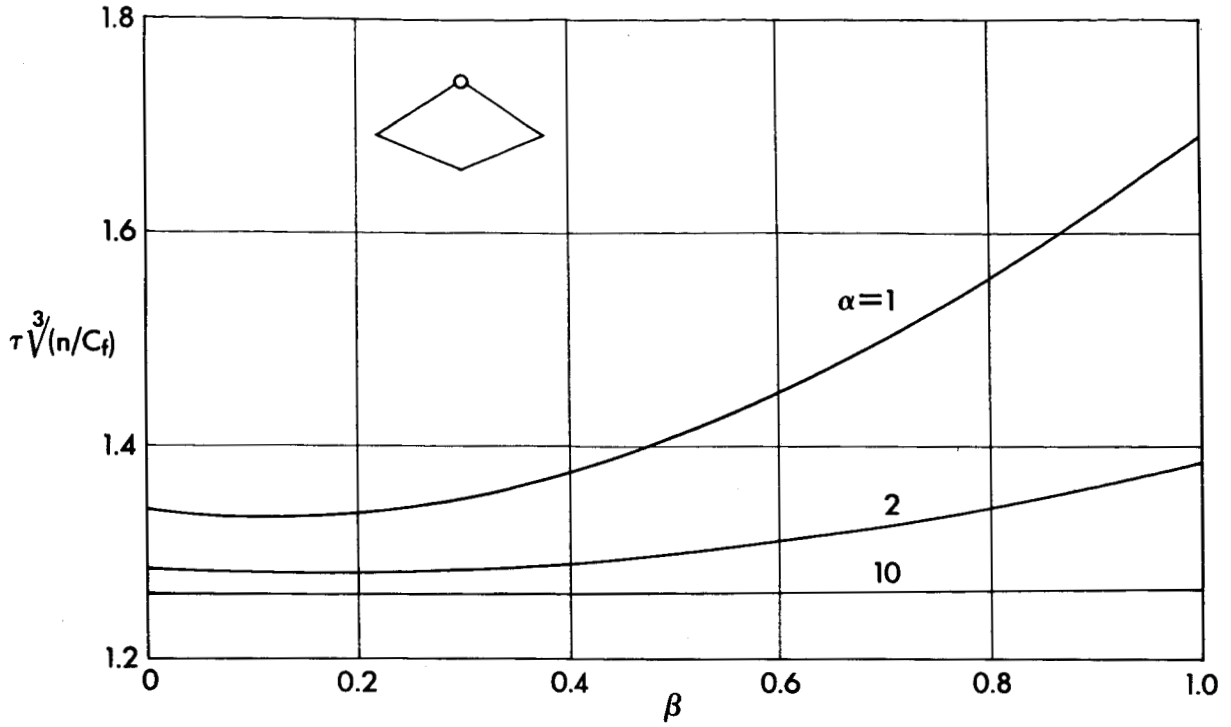

Fig. 25 Optimum thickness ratio.

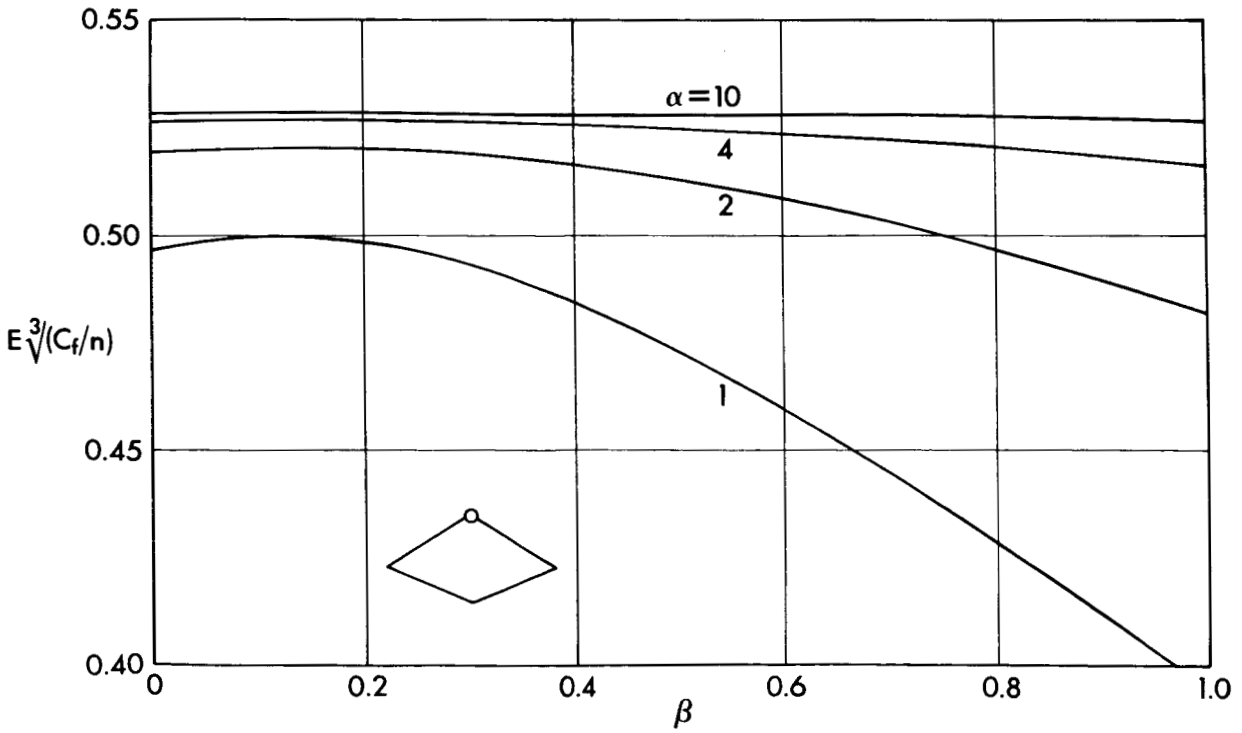

Fig. 26 Maximum lift-to-drag ratio.

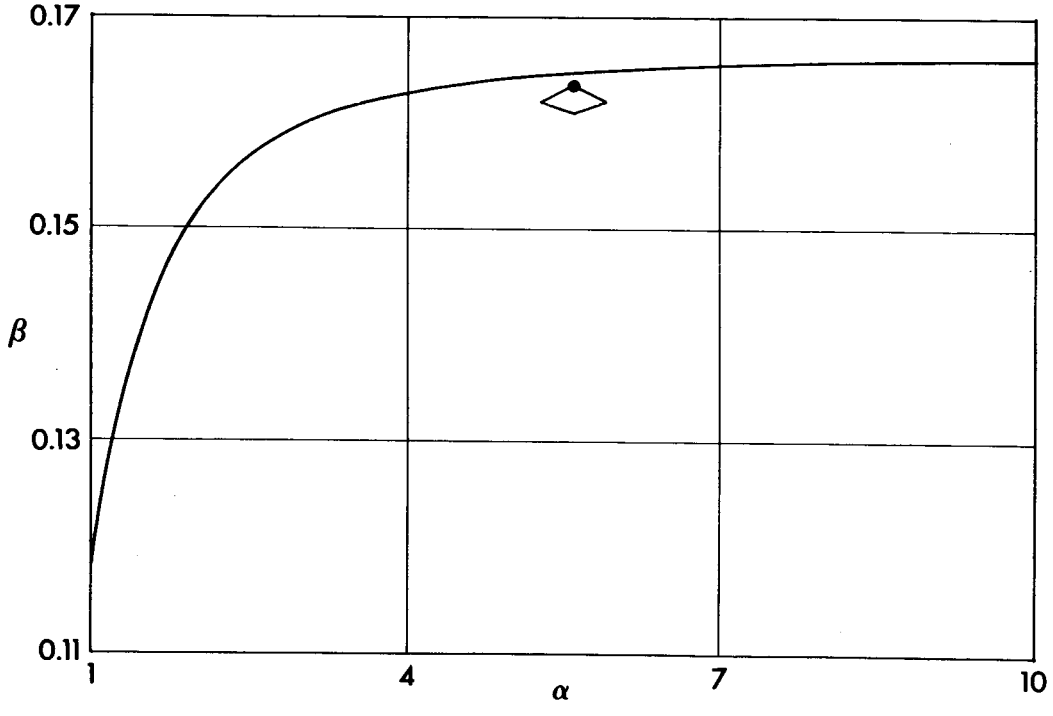

Fig. 27 Optimum value of the parameter β.

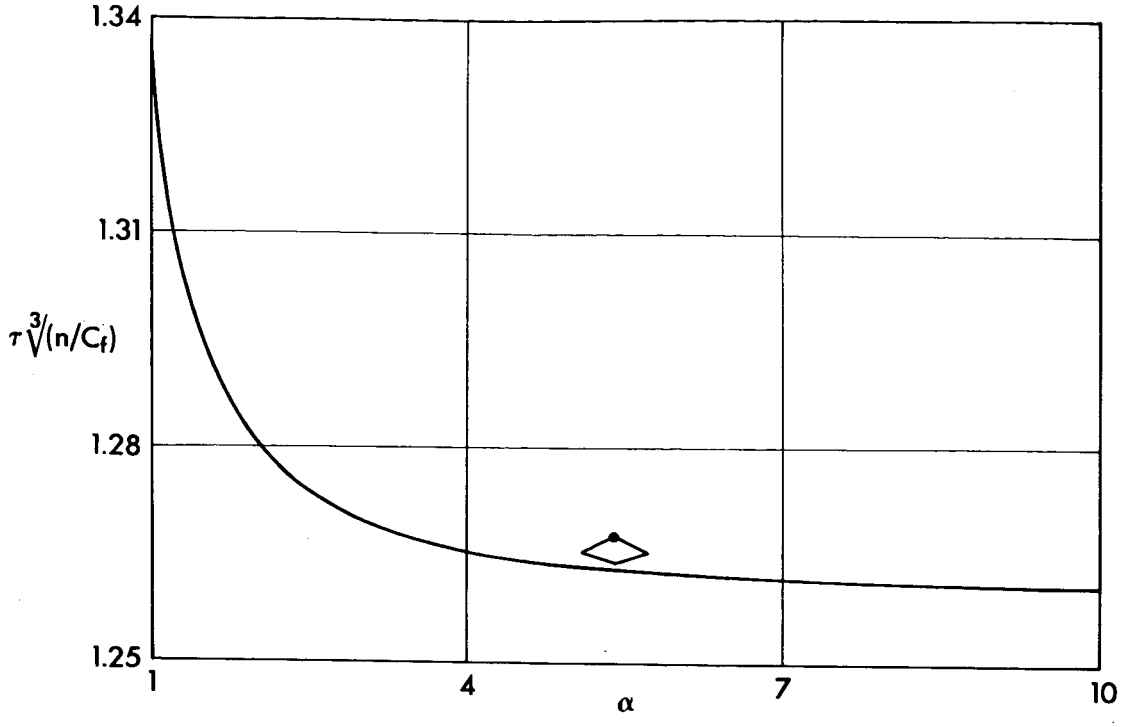

Fig. 28 Optimum thickness ratio.

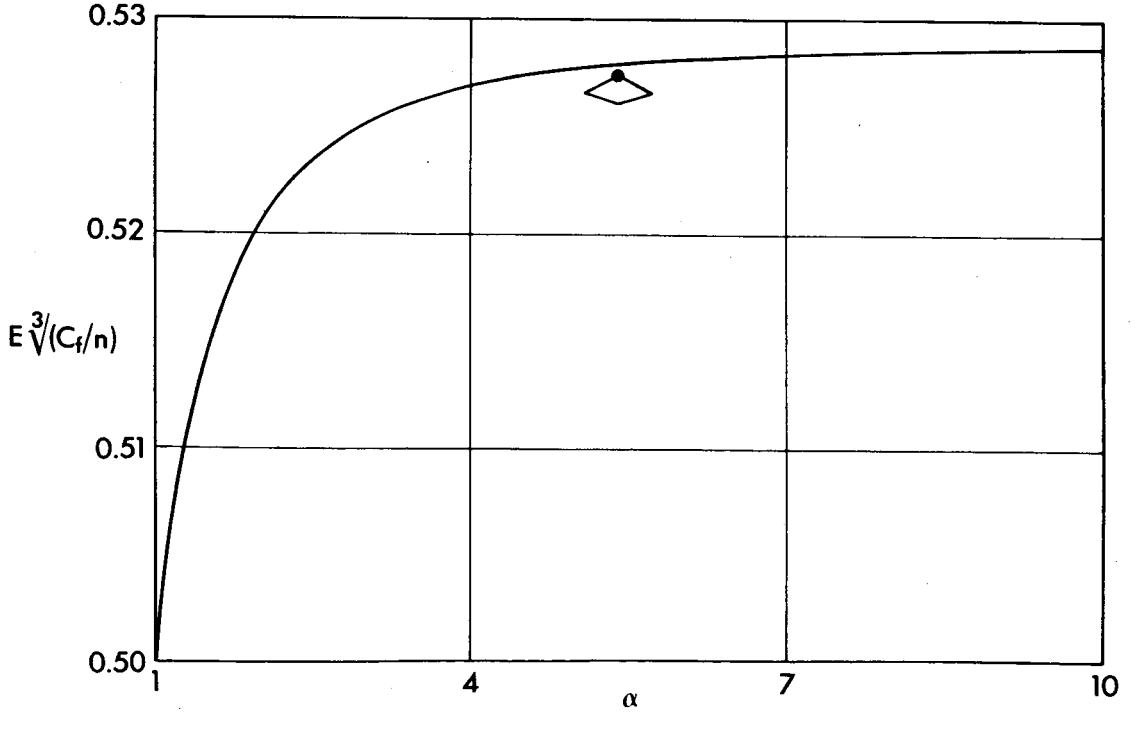

Fig. 29 Maximum lift-to-drag ratio.

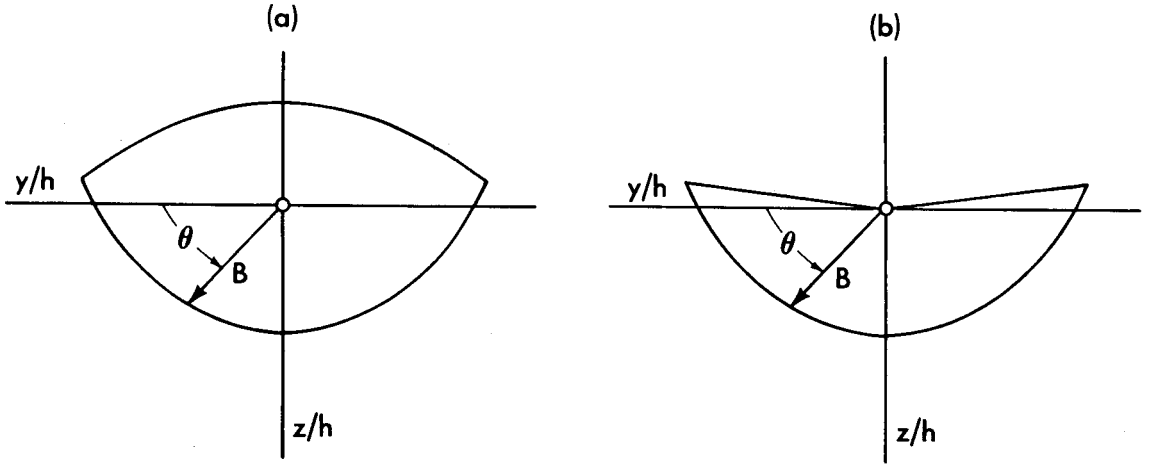

Fig. 30 Cross sections with the apex below the maximum width line.

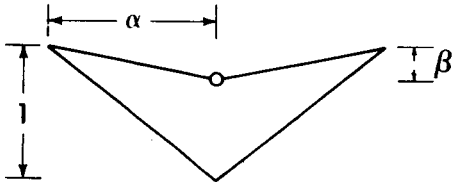

Fig. 31 Particular cross section.

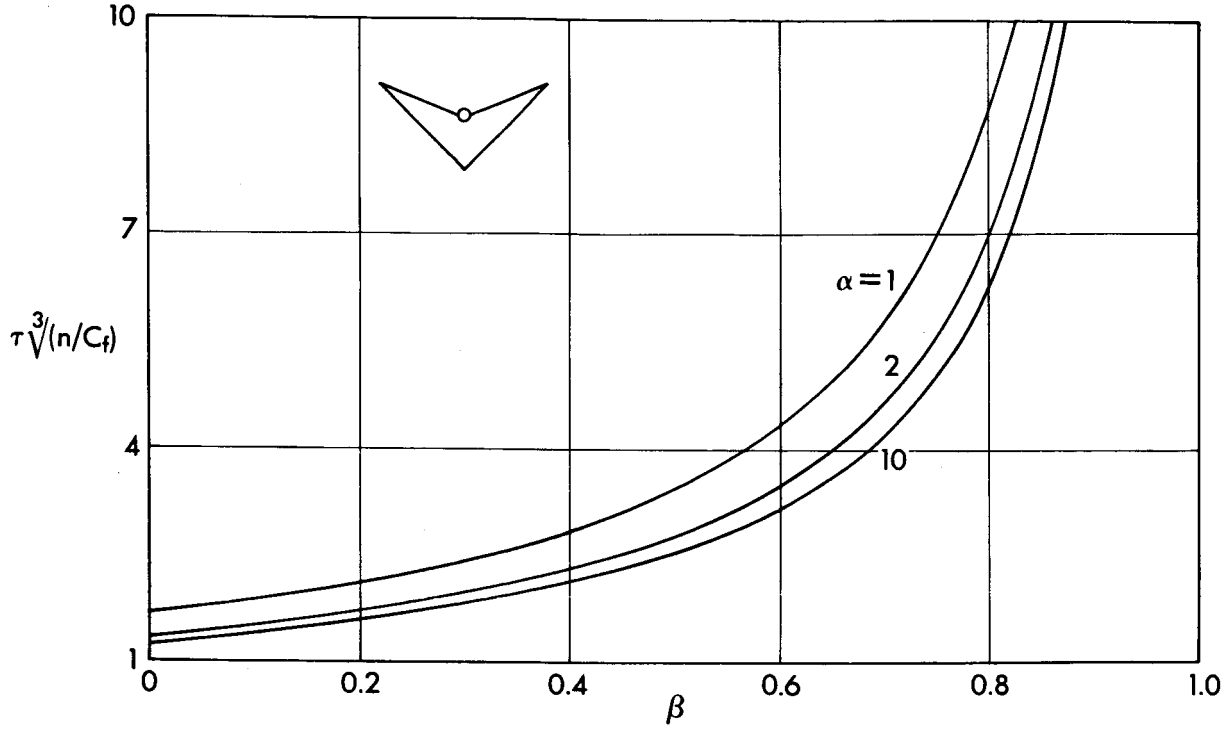

Fig. 32 Optimum thickness ratio.

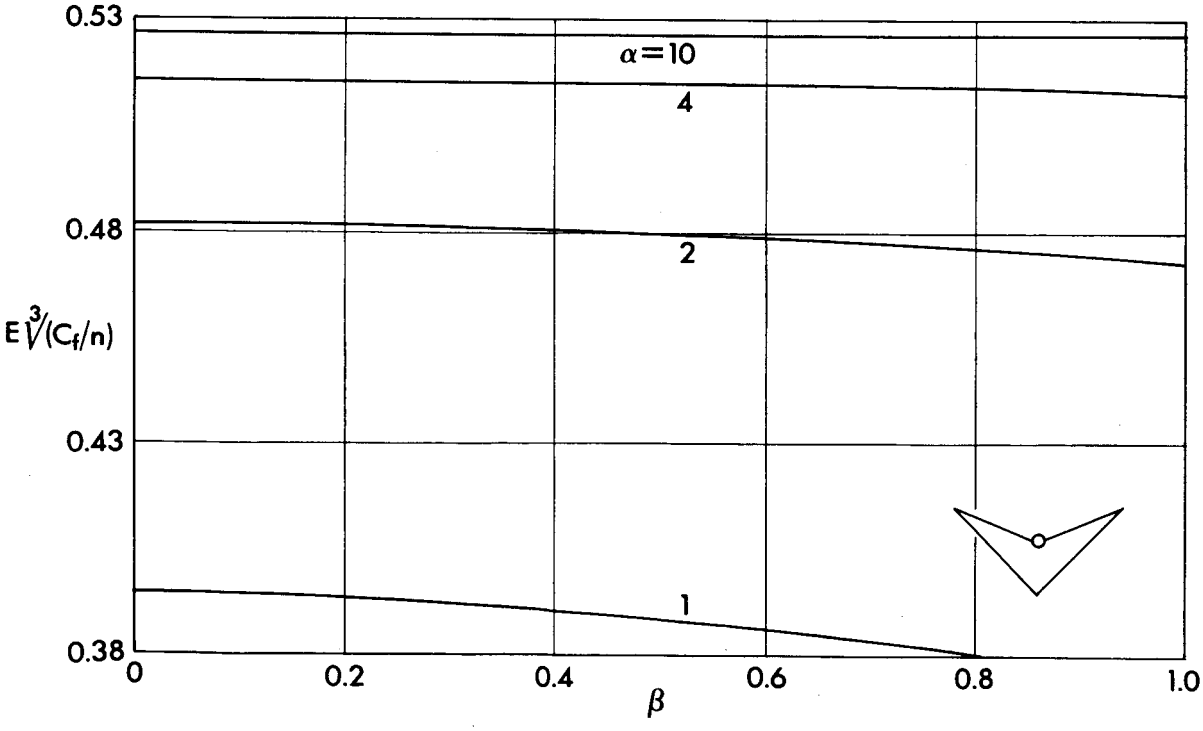

Fig. 33 Maximum lift-to-drag ratio.